SLOTLINE COMPONENTS

Slotline components, just as the term implies, are the microwave circuit components consisting of slotlines and combinations of slotlines and other transmission lines such as microstrip and coplanar waveguide (CPW).

Slotline is a nontransverse electromagnetic (non-TEM) uniplanar transmission structure using a single slot etched on a dielectric-supported layer of metal without a backside ground plane (1). The slotline configuration is useful in circuits requiring high-impedance lines, series stubs, short circuited ends, and easy series and shunt connections of passive and active solid-state devices without via holes. With its advantages of small size, light weight, and low cost, slotline has emerged as an alternative transmission line for applications in microwave integrated circuits (MICs) and monolithic microwave integrated circuits (MMICs). These circuits include filters, couplers, ferrite devices, and other components as well as complete circuits.

Slotline can also be combined with microstrip and CPW for many circuit applications. These types of hybrid combinations allow flexibility in the design of MIC and MMIC components. For example, a wide range of line impedance, compact circuit structure, easier device mounting, and better integration are achievable in printed form. These features have led to many novel circuits like hybrid couplers, magic-Ts, oscillators, mixers, receivers, antennas, and so forth. In spite of these numerous advantages and uses, the description of the slotline components is generally hidden in many papers and books. Because of limited space this article is merely intended to present the typical slotline components. By outlining their basic operation principle, an overview of the general function of the important circuit components is given. The basic characteristics of slotlines, such as wavelength, characteristic impedance, quality factor, and its discontinuities, can be found in SLOTLINES.

This article first discusses the fundamental slotline elements such as various T-junctions, resonators, and transitions. After these general topics, several kinds of passive slotline integrated circuits are presented through a discussion of filters, hybrid couplers, and nonreciprocal devices. Finally, the applications of slotline to solid-state integrated circuits, that is mixers, oscillators, modulators, and frequency doublers, are described. These applications are supported by real circuit demonstrations and actual circuit performances. The implementation of solid-state devices for the tuning and switching of resonances is also discussed.

BASIC SLOTLINE CONFIGURATIONS

Slotline Tee Junctions

Slotline tee junctions appear very frequently in slotline-microstrip circuits (double-sided MICs) and slotline-CPW circuits (uniplanar MICs). Figure 1 shows the physical configurations of various slotline T-junctions. In accordance with the input and output transmission lines, the T-junctions can be classified into parallel and series types. The parallel T-junctions [Fig. 1(a), (b), and (c)] require the unbalanced line (coaxial line, microstrip, or CPW) as an input transmission line, while the series T-junctions [Fig. 1(d), (e), and (f)] require the balanced line (slotline). It is necessary to note that the CPW (without bonding wire) in Fig. 1(f) is the coupled slotline which operates in coupled-slotline mode (also called the CPW

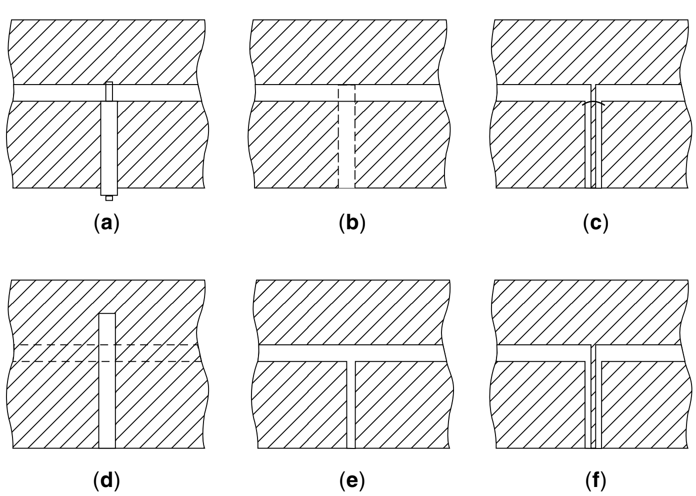

Figure 1. Various slotline T-junctions: (a) coax-slot T; (b) microstrip-slotline T; (c) CPW-slotline T; (d) slotline-microstrip series T; (e) slotline T; and (f) CPW (even mode)-slotline series T. Solid lines show slotlines and CPW lines on the substrate. Dotted lines show microstrip lines on the back side of the substrate.

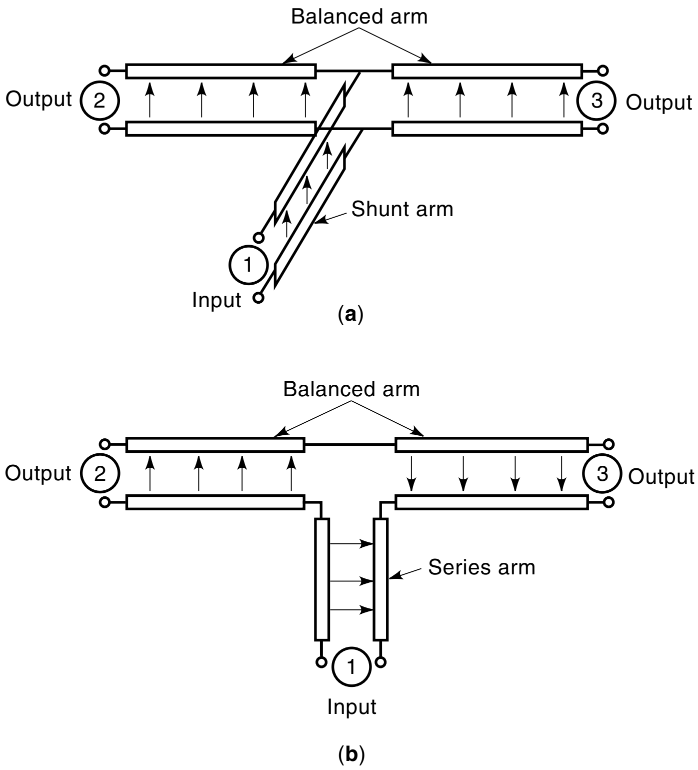

Figure 2. Equivalent transmission line models of the slotline T-junctions of Fig. 1: (a) shunt model of the slotline T-junctions for Fig. 1(a), (b), and (c); (b) series model of the slotline T-junctions for Fig. 1(d), (e), and (f).

even mode). Figure 2 shows equivalent transmission line circuits and schematic expression of the circuit behavior for the parallel and series T-junctions of Fig. 1. The arrows in the figure indicate the electric field distribution in the circuits. For the parallel tee as shown in Fig. 2(a) when an incident wave fed to port 1 propagates through the input line, at the T-junction it will divide into two components that both arrive in phase at ports 2 and 3. For series tee as shown in Fig. 2(b) when an incident wave fed to port 1 propagates through the input line, at the T-junction it will divide into two components that arrive at ports 2 and 3 with a 180° phase difference.

Both series and parallel T-junctions can be combined to realize hybrid circuits and balanced circuits. In addition, it is worth mentioning that the T-junctions in Fig. 1(c), (e), and (f) can be fabricated using only one side of the substrate. This is a great advantage in developing uniplanar MICs as discussed in later sections.

Slotline Transitions

To test slotline circuits, a transition between slotline and the measuring transmission lines is necessary. A coax-slotline transition is first used for this purpose. To increase the application of slotlines transitions from slotline to other transmission lines are also useful. Such transitions are slotline to microstrip and slotline to CPW. These three types of transitions discussed in this section are based on the slotline T-junctions of Fig. 1. Interested readers may refer to Refs. 1–5.

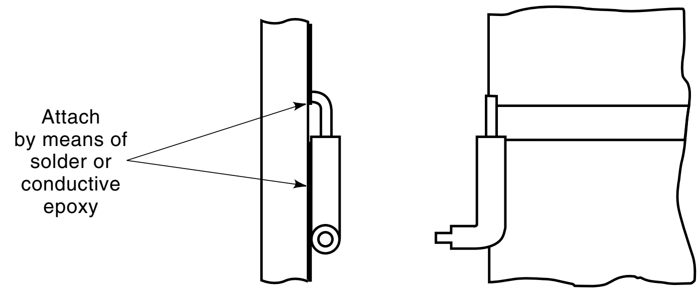

Figure 3. A coax-slotline transition that is a wide-band transition between slotline and miniature-cross-section coaxial line. (From Ref. 2 with permission, © 1969 IEEE.)

Coax-Slotline Transitions. Figure 3 shows a commonly used coax-slotline transition reported by S. B. Cohn (2) in 1969. It consists of a miniature semirigid coaxial line placed at the end of an open slotline. Both the inner and outer conductors of the coaxial line are electrically connected (with solder or epoxy) to the conductive plating on the two sides of the slot. As mentioned above, this transition is based on the coax-slotline T-junction of Fig. 1(a). This T-junction works like a power divider with an open termination at one of its output ports. The transition was constructed with a slot width of 0.79 mm on a 1.57 mm thick Trans-Tech D-16 substrate ($\epsilon_r = 16.3$). The slotline impedance corresponding to these dimensions is about 75 Ω. The voltage standing-wave ratio (VSWR) looking into the 50 Ω coaxial line was less than 1.2 over a 500 MHz bandwidth at 3 GHz.

Microstrip-Slotline Transitions. Microstrip-slotline transitions are transformers between unbalanced and balanced lines. The majority of transitions are based on the well-known concept of Marchand balun. Since 1969 when the first microstrip-slotline transition was reported, various microstrip-slotline transitions have been developed for double-sided MICs that use a combination of microstrip and slotlines on both sides of the substrate. Various microstrip-slotline transitions are shown in Fig. 4. In Fig. 4(a–e), the transitions consist of

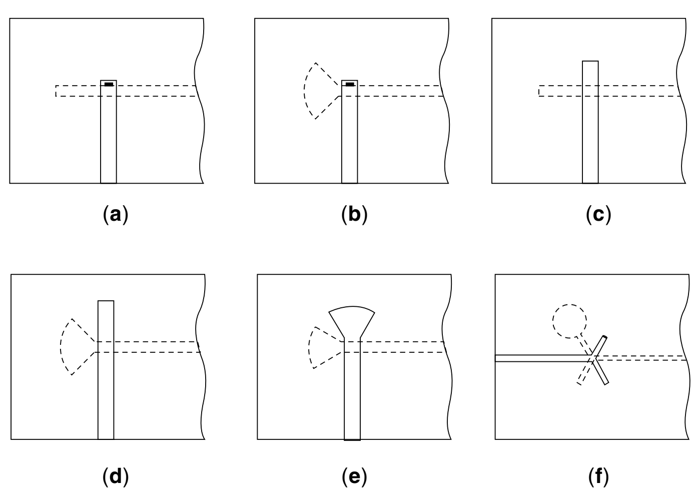

Figure 4. Circuit configurations of microstrip-slotline transitions with different terminations: (a) and (c) transitions with uniform impedance stubs; (b), (d), and (e) transitions with nonuniform impedance stubs; (f) double Y-junction microstrip-slotline transition. Solid lines show microstrip lines on the substrate. Dotted lines show slotlines on the back side of the substrate.

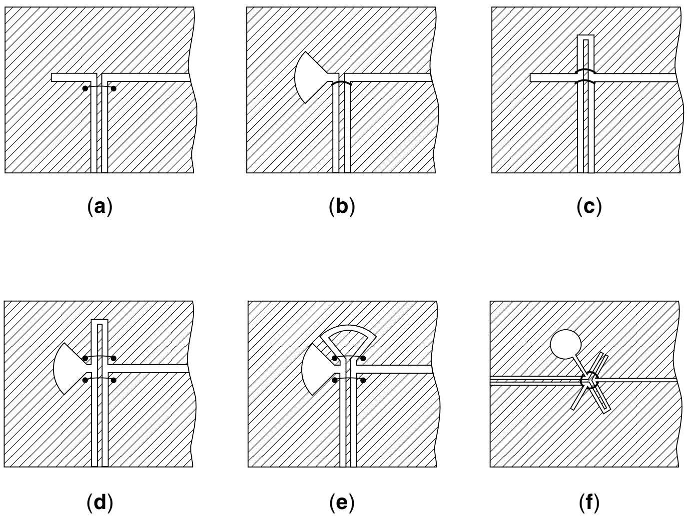

Figure 5. Circuit configurations of CPW-slotline transitions with different terminations: (a) a CPW short with a uniform slotline short stub; (b) a CPW short with a nonuniform slotline short stub; (c) a uniform CPW open stub with a uniform slotline short stub; (d) a uniform CPW open stub with a nonuniform slotline short stub; (e) a nonuniform CPW open stub with a nonuniform slotline short stub; (f) a uniplanar double Y-junction CPW-slotline transition.

uniform and nonuniform impedance stubs as well as soldered and virtually shorted microstrip stubs. They are based on the microstrip-slotline T-junctions of Fig. 1(b) and (d) with a different termination at one of the T-junction output ports. Modeling and experimental investigation on these transitions was carried out by Schuppert (3). The back-to-back connection of two transitions shown in Fig. 4(e) has a bandwith of approximately one decade. The bandwidth of a single transition will obviously be larger than that of two transitions. It was also found that the transition with a microstrip short shown in Fig. 4(b) has a larger bandwidth than the transition with a microstrip open stub. However, its implementation needs a via-hole grounding that may sometimes be difficult. The transition shown in Fig. 4(f) is not based on the type of Marchand baluns, but on a six-port junction. Although this transition has good performance over a broadband from 2 GHz to 9 GHz, it occupies more substrate space.

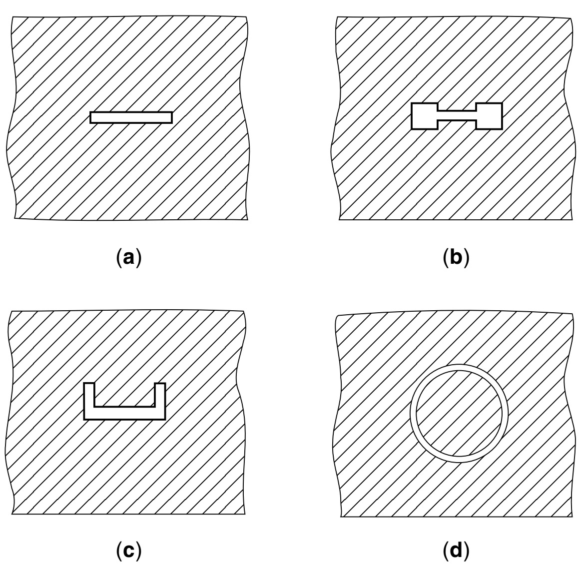

Figure 6. Slotline resonators: (a) rectangle; (b) rectangle with capacitive loading; (c) bent rectangle; (d) ring.

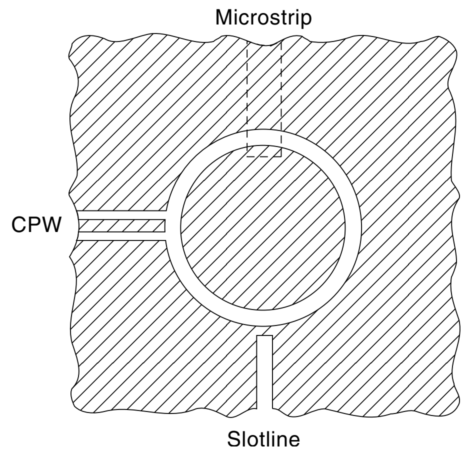

Figure 7. Circuit configuration of slotline ring resonator with different coupling schemes: microstrip-fed, CPW-fed, and slotline-fed slotline rings. (From Ref. 9 with permission, © 1993 IEEE.)

CPW-Slotline Transitions. Coplanar waveguide and slotline are the fundamental transmission lines and are useful in uniplanar MICs and MMICs. CPW-slotline transitions are realized on one substrate side without metallization on the backside. This feature can significantly reduce the substrate processing complexity and consequently the cost. To fully utilize the advantages of uniplanar structures the transition between CPW and slotline is necessary. Extensive study and modeling have been carried out to investigate various transition configurations. CPW-slotline transitions that are equivalent to the microstrip-slotline transitions of Fig. 4 are shown in Fig. 5. They have been evaluated experimentally (4) and theoretically (5). The transition in Fig. 5(a) is based on the CPW-slotline T-junction of Fig. 1(c). One of the output ports of the T-junction is terminated in a quarter-wavelength slotline short stub which provides tuning capability. To improve the

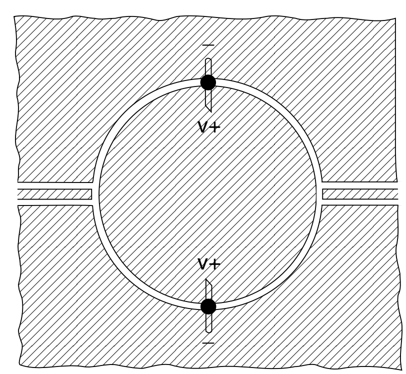

Figure 8. Varactor-tunable slotline ring resonator with CPW feeds: Two 50 Ω CPW lines feed an 85 Ω slotline ring through a 0.05 mm series gap. The ring has a mean radius of 11.26 mm and uses a 0.5 mm slotline on a 0.63 mm thick RT-Duroid 6010 substrate ($\epsilon_r = 10.5$). (From Ref. 7 with permission, © 1993 IEEE.)

bandwidth, the short stub has been replaced by a radial slotline stub in Fig. 5(b). Figures 5(c–e) show the transition where a quarter-wavelength CPW open stub or a CPW radial stub is used instead of CPW shorts of the transitions in Fig. 5(a) and (b). Overall, the transition with nonuniform radial stubs has larger bandwidth than that with uniform stubs. Experimental investigations of these transitions show that the transition in Fig. 5(b) gives the best performance with a 5.2 : 1 bandwidth and insertion loss of less than 1 dB. Other transitions of Fig. 5(a), (c), (d), and (e) have a bandwidth ranging from 1.6 : 1 to 4.1 : 1. Similar to the microstrip-slotline transition in Fig. 4(f), the transition shown in Fig. 5(f) uses a double-Y junction between CPW and slotline. This transition has better performance than other uniplanar transitions except for its need for more substrate room. The measured results of this transition show less than a 1.6 VSWR and 0.7 dB insertion loss for a bandwidth ratio of 6 : 1.

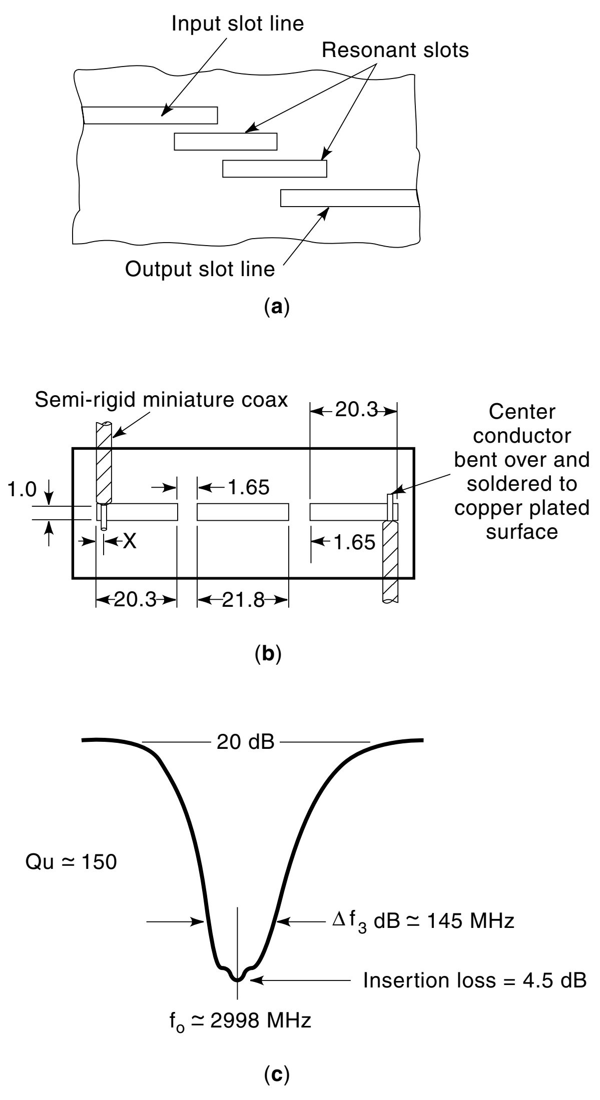

Figure 9. Slotline bandpass filters: (a) configuration of quarter-wavelength-coupled slot-resonator filter; (b) circuit configuration of end-coupled slot-resonator filter; (c) bandpass response of (b). (From Ref. 8 with permission, © 1970 IEEE.)

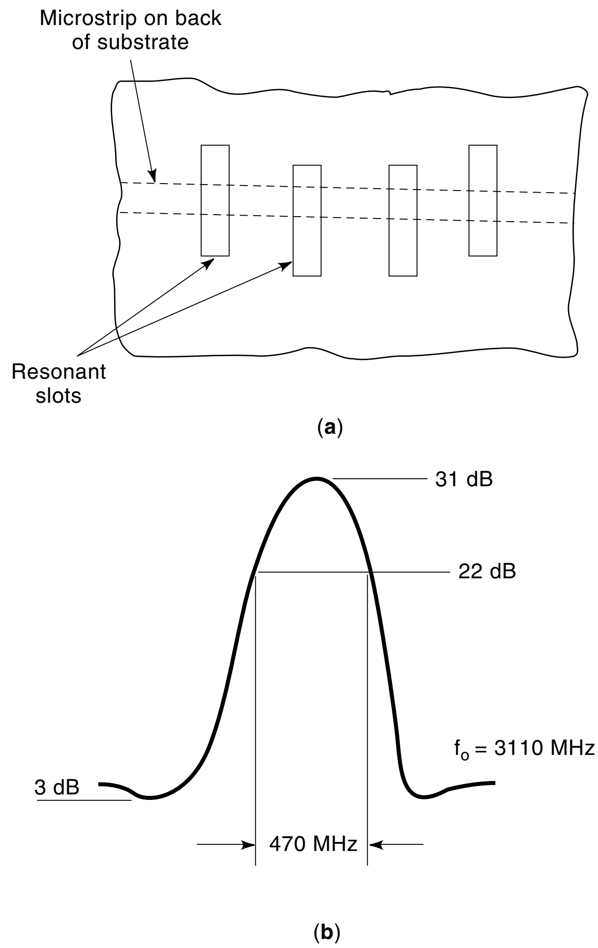

Figure 10. (a) Configuration and (b) characteristic response for slotline bandstop filter. (From Ref. 8 with permission, © 1970 IEEE.)

Slotline Resonators

Slotline resonators are basic elements served as wavelength measurements, filters, and other MIC components. The slotline resonator is an uniplanar structure etched on one substrate side without back metallization. As shown in Fig. 6(a), a half-wavelength rectangular slot is a typical resonator used exclusively for the various filters. If necessary, the rectangular resonator slot can be made by capacitive loading over a portion of its length to reduce its resonator frequency as in Fig. 6(b) or by bending it as in Fig. 6(c) to conserve length with relatively little effect on the resonant frequency.

The slotline ring resonator as shown in Fig. 6(d) is widely used in many circuit applications (6). Coupling between the feed lines and slotline ring can be the following three types: microstrip coupling, CPW coupling, and slotline coupling. Figure 7 shows these three possible coupling schemes. The microstrip coupling is a capacitive coupling. The length of input and output microstrip coupling stubs can be adjusted to optimize the loaded Q values. However, less coupling may effect the coupling efficiency and cause higher insertion loss. The trade-off between the loaded Q and coupling loss depends on the application. CPW coupling is also a capacitive coupling and is formed by a small coupling gap between the CPW feed lines and the slotline ring. The loaded Q value and insertion loss are dependent on the gap size. The smaller gap size will cause a lower loaded Q and smaller insertion loss. Unlike microstrip and CPW couplings, the slotline ring coupled to slotline feed is an inductively coupled ring resonator. The metal gap between the slotline ring and slotline feed is for the coupling of magnetic field energy. Therefore, the maximum electric field points of this resonator are opposite to those of the capacitively coupled slotline ring resonators.

The last two types of slotline ring resonators are truly coplanar and also allow easy series and shunt device mounting. Varactor diodes can be incorporated into the ring resonators to make the resonant frequencies electronically tunable. For example, Fig. 8 shows varactor-tunable slotline ring resonator (7). The varactors located at 90° and 270° along the ring tune the even modes of the resonator and allow a second mode electronic tuning bandwidth of more than 22% from 3.13 GHz to 4.07 GHz. The frequency responses of the circuit agree very well with those calculated using a distributed transmission line model.

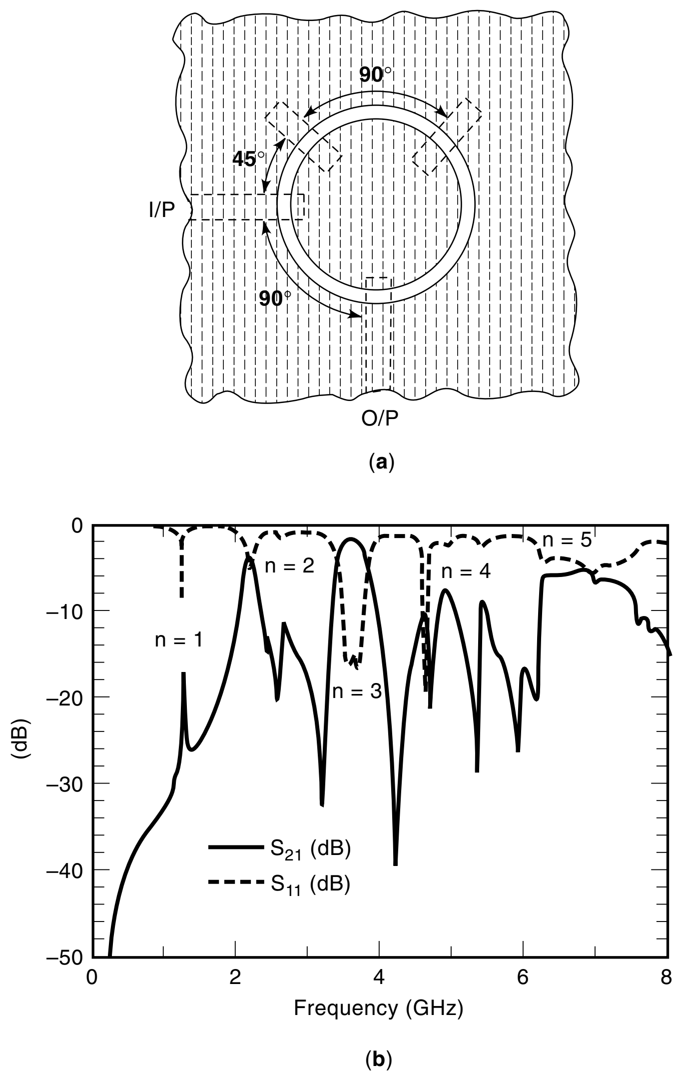

Figure 11. Slotline ring dual-mode bandpass filter: (a) physical circuit etched on a RT-Duroid 6010 substrate (ϵ_r = 10.5, h = 0.63 mm); (b) measured frequency responses of insertion loss and return loss. (From Ref. 9 with permission, © 1993 IEEE.)

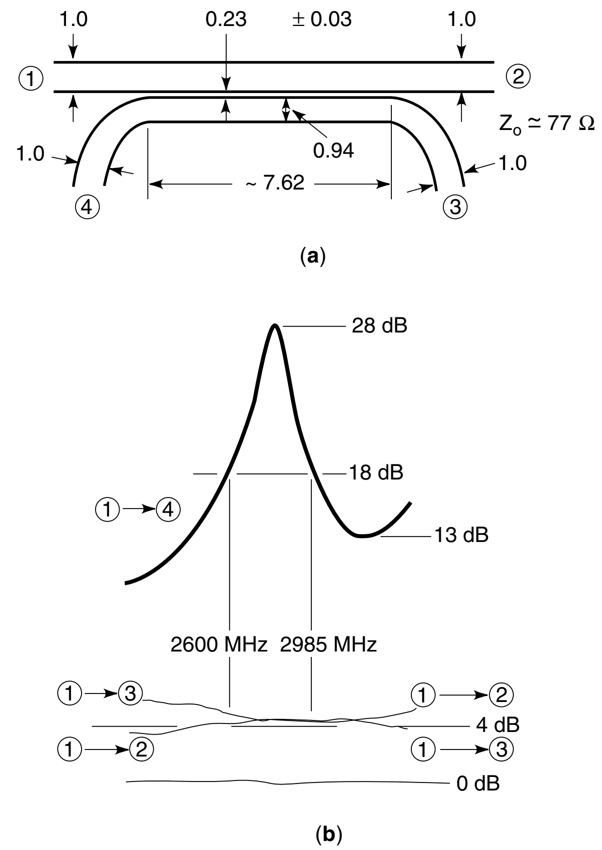

Figure 12. Parallel coupled slotline coupler: (a) physical configuration (all dimensions in millimeters); (b) measured frequency responses of insertion loss and return loss. (From Ref. 8 with permission, © 1970 IEEE.)

PASSIVE SLOTLINE COMPONENTS

Based on the discussion of the fundamental slotline elements in the previous section, this section describes passive slotline components such as filters, magic-Ts, and various hybrid couplers in detail.

Slotline Filters

The slotline on high dielectric substrate provides a microwave medium for fabricating bandpass and bandstop filters that have been used in MICs. In 1970, Mariani and Agrios (8) reported two types of bandpass filters using the end-coupled and quarter-wave-coupled resonant slots as shown in Fig. 9. For example, a three-resonator end-coupled bandpass filter was designed and constructed on a D-16 substrate (ϵ_r = 16.3, h = 1.6 mm). Important dimensions are shown in Fig. 9(b). The distance X was adjusted experimentally for matching external loading of the end resonators. The measured response as shown in Fig. 9(c) was in reasonable agreement with the design goals. The filter had a 3 dB bandwidth of 145 MHz centered at 2998 MHz. The insertion loss, including the losses of the coax-slotline transition, was 4.5 dB which corresponds to Q_u of about 150.

Slotline bandstop filters are easily implemented by using the combination of slotline and microstrip as shown in Fig. 10(a). The slot resonators are etched on the ground plane of

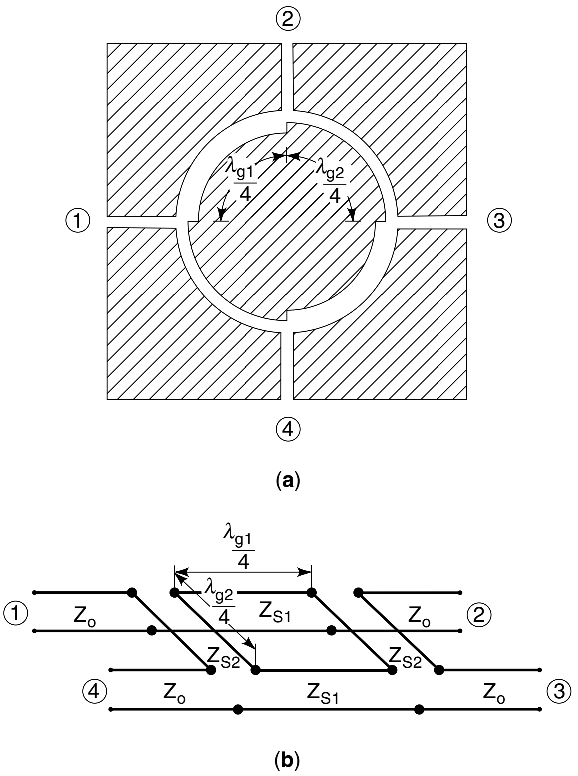

Figure 13. Slotline branch-line coupler: (a) physical configuration; (b) equivalent transmission line model. Two branch arms are connected to the through arms in series. (From Ref. 12.)

the microstrip line which acts as the terminating line. Such a two-resonator bandstop filter was built on a 1.6 mm thick D-16 substrate using the same configuration in Fig. 10(a). The slots had an impedance of 85 Ω, approximately $\lambda_g/2$ long, and a separation of $3\lambda_m/4$ (λ_m is the wavelength of the microstrip line). Figure 10(b) shows a rejection response of about 15% at the 20 dB level for the filter.

Another application of slotline-microstrip combination in filters is the microstrip-fed slotline dual-mode bandpass filter (9). By using microstrip tuning stubs on the backside of the slotline ring at 45° and 135°, the dual resonant mode can be excited. Figure 11(a) shows the physical configuration of the slotline dual-mode bandpass filter. The microstrip feedlines located at 0° and 270° are used to extract both sine and cosine resonant modes which are orthogonal to each other in the ring structure. Figure 11(b) shows the measured insertion and return loss as for the slotline dual-mode bandpass filter with mode number $n = 3$. The dual-mode filter has a 12% bandwidth at the center frequency of 3.5 GHz, a stopband attenuation of more than 30 dB, and a sharp gain slope transition. Compared with the microstrip dual-mode filter, the slotline dual-mode filter has a better in-band and out-band performance. Also, the slotline ring dual-mode filter has the advantages of flexible tuning and ease of adding series and shunt devices.

Ferrite Devices

Slotline application to ferrite devices was reported in 1969 when the slotline was just introduced as an alternative transmission line for microwave integrated circuits (10). Based on the existence of an elliptically polarized magnetic field, slotline was used for the design of planar ferrite phase shifters, circulators, and isolators. The design procedure for the slotline ferrite devices is the same as that for the microstrip line. However, the experimental results reported so far indicate that the performance of the slotline ferrite devices is not superior to those using a microstrip line.

Slotline Branch-Line Couplers, Hybrid Couplers, and Magic-Ts

Hybrids and couplers form an indispensable component group in modern MIC and MMIC technology. With the inventions of new planar transmission lines like CPW, slotline, coplanar stripline (CPS), coupled microstrip-slot lines, and their derivatives, many types of hybrids and couplers have been developed over the past few decades. This growth is due to the rapidly expanding applications in wireless communications, radar, sensors, electronic warfare, and space technology.

This section describes different types of slotline branch-line couplers, hybrid couplers, and magic-Ts and their applications.

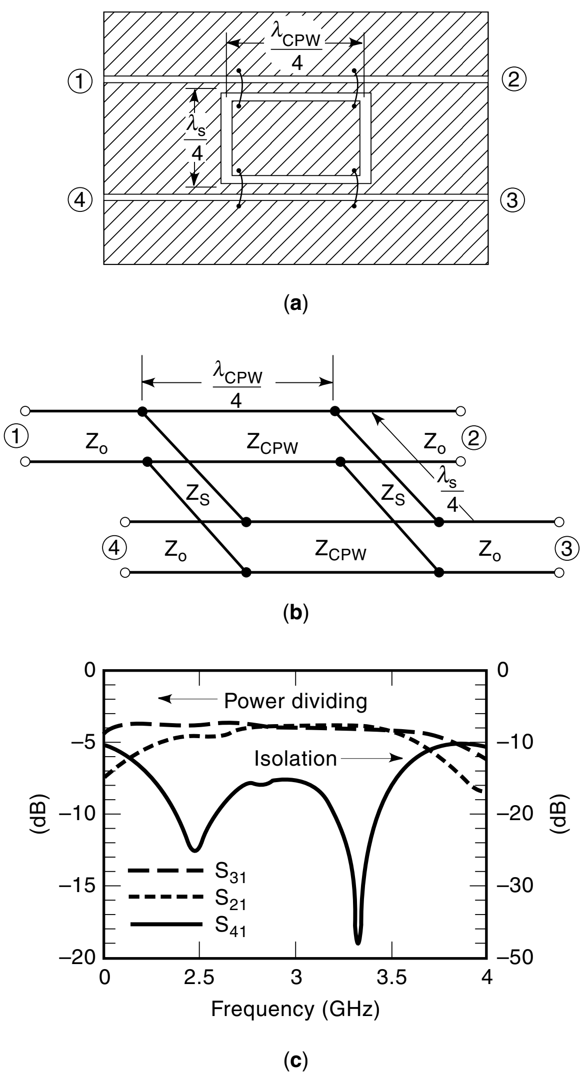

Figure 14. Uniplanar slotline-CPW hybrid branch-line coupler: (a) physical configuration; (b) equivalent transmission line model; (c) measured frequency responses of power dividing and isolation. (From Ref. 4 with permission, © 1993 IEEE.)

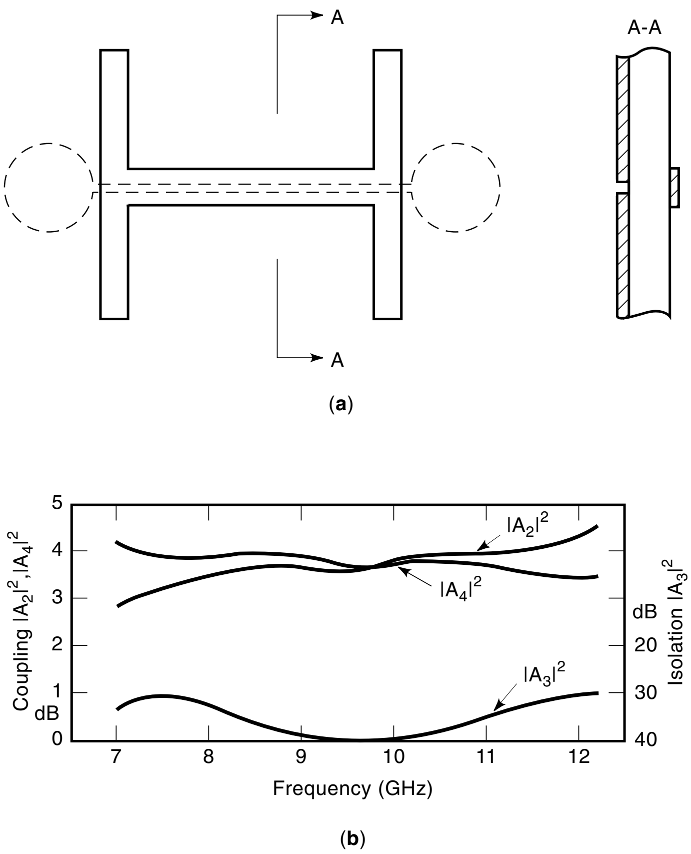

Figure 15. Microstrip-slot de Ronde's coupler: (a) physical configurations (left: top view; right: side view); (b) measured performance for the coupler's couplings and isolation. (From Ref. 14 with permission, © 1974 IEEE.)

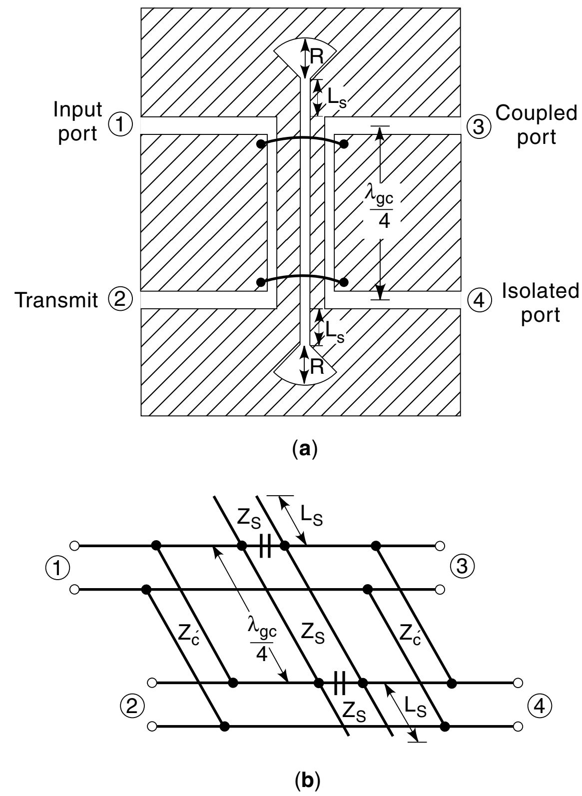

Figure 16. Uniplanar de Ronde's CPW-slot directional coupler: (a) physical configuration; (b) equivalent transmission line model. (From Ref. 16 with permission, © 1995 IEEE.)

Parallel Coupled Slotline Directional Coupler. The first attempt in fabricating a parallel coupled slotline coupler was successful by Mariani and Agrios in 1970 (8). The coupler used a D-16 dielectric substrate ($\epsilon_r = 16.3$, h = 1.6 mm) with aluminum tape metallization. The actual circuit dimensions are shown in Fig. 12 along with the measured results. Unlike the backward coupling (electric coupling) in the case of parallel microstrip-coupled line couplers, the coupling of the coupled slotline coupler is magnetic coupling in the forward direction as in the case of the waveguide narrow-wall coupler. As shown in Fig. 12(b), the coupler had a 4 dB coupling (3 dB is ideal coupling) over a wideband of about 600 MHz. The insertion loss was nearly 1 dB which includes the coax-slotline transitions. The isolation bandwidth of 18 dB was 400 MHz centered at 2.8 GHz (about 14% bandwidth). According to their experiments, the reporters indicated that: 1) the performance of slotline coupler could be improved by optimizing the various important physical dimensions such as the separation, coupling length, and slot width, and 2) a 3 dB coupling implementation in using parallel coupled slotline is quite practical and a wider bandwidth of 40% is possible.

Uniplanar Branch-Line Couplers. It is well known that microstrip branch-line couplers are basic components in applications such as power dividers, balanced mixers, frequency discriminators, and phase shifters. The concept and analysis of the branch-line couplers can be found in many microwave textbooks. This section presents two uniplanar branch-line couplers using slotline and CPW structures (4). The design technique for the slotline branch-line coupler uses series branch lines. The design technique for the slotline-CPW hybrid branch-line coupler uses shunt branch lines.

Figure 13(a) shows the physical configuration of the slotline two-branch-line coupler (11). For the case of 3 dB coupling, when a signal is applied to port 1 the outputs appear at ports 2 and 3 and are equal in amplitude and differ in phase by 90°. Port 4 is the isolation port. Figure 13(b) shows the equivalent transmission line model of the slotline branch-line coupler. The through arms and branch arms are con-

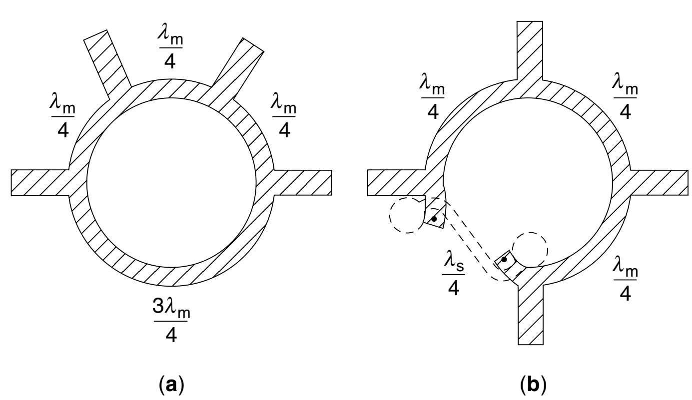

Figure 17. Circuit configurations of microstrip hybrid-ring couplers: (a) rat-race hybrid-ring coupler using microstrip lines only; (b) reverse-phase hybrid-ring coupler using a $\lambda_s/4$ slotline section instead of the $3\lambda_m/4$ microstrip line in (a).

nected in series. The corresponding line characteristic impedances of the slotline through and branch arms, in terms of the termination impedance Z_0, can be expressed as

$$Z_{S1} = \sqrt{2}Z_0; \quad Z_{S2} = Z_0 \tag{1}$$

where Z_{S1} is the characteristic impedance of the slotline through arms, and Z_{S2} is the characteristic impedance of the slotline branch arms.

The measured performance is summarized below. The amplitude imbalance of 1 dB is within a bandwidth of less than 20% at the 3 GHz center frequency. The measured isolation between ports 1 and 4 is greater than 30 dB at the center frequency of 3 GHz. A computer program based on the equivalent transmission line model of Fig. 13(b) was developed and was used to analyze the circuit. The calculated results agree very well with the measured results.

Another type of uniplanar branch coupler is a slotline-CPW hybrid branch-line coupler consisting of a rectangular slotline ring coupled with two parallel slotline feeds. The uniplanar hybrid branch-line coupler is dual to the slotline branch-line coupler in Fig. 13(a). Figure 14(a) shows the physical configuration of the branch-line coupler (13). The two CPW through arms are fed by input and output slotlines and connected by two slotline shunt branch arms. The equivalent transmission line model of the coupler is shown in Fig. 14(b). Adding bonding wires at the circuit's discontinuities is important to prevent the coupled slotline mode from propagating

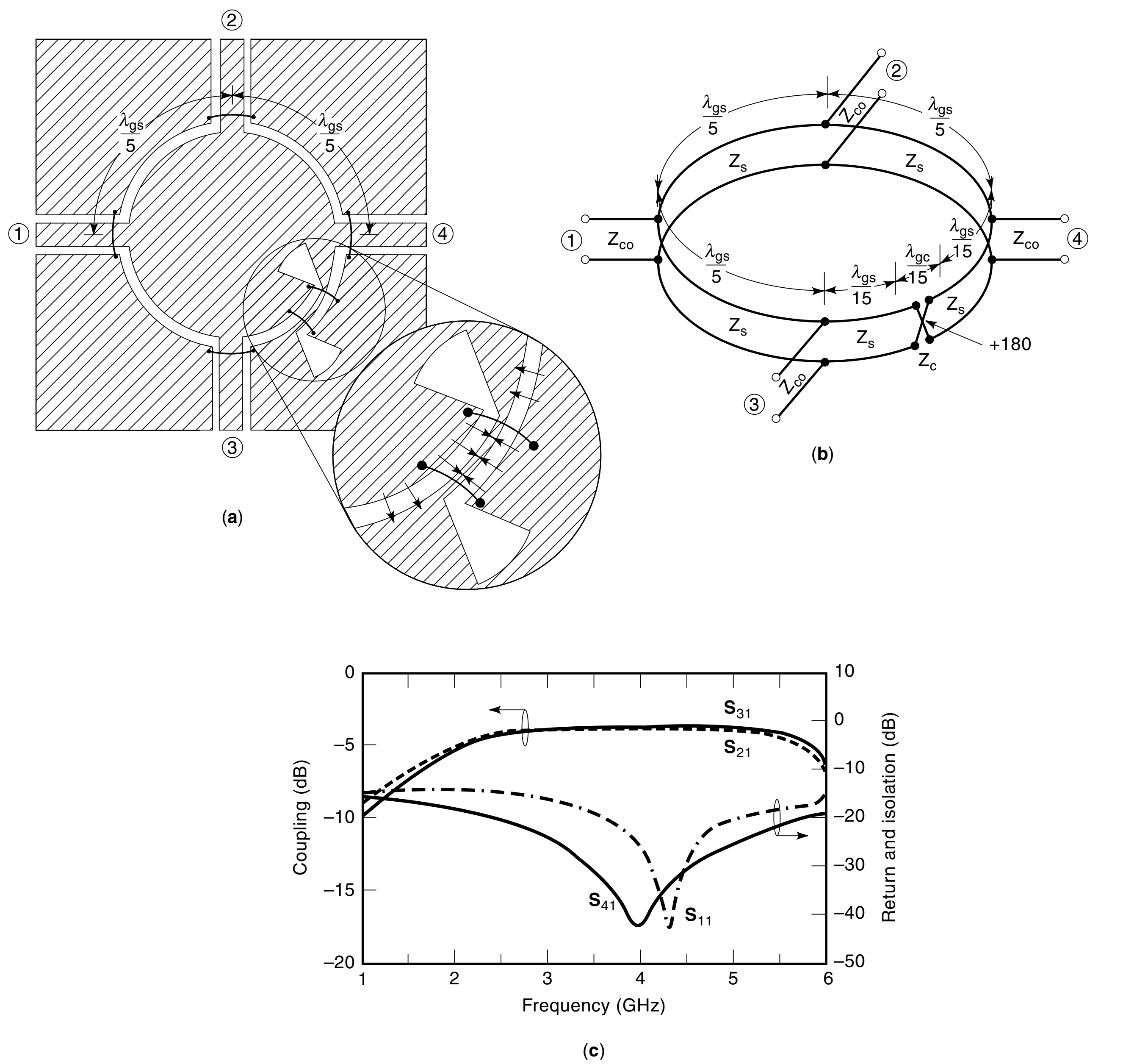

Figure 18. Uniplanar reduced-size reverse-phase hybrid-ring coupler: (a) circuit configuration; (b) equivalent transmission line model; (c) measured frequency responses of coupling, return loss, and isolation. (From Ref. 17 with permission, © 1995 IEEE.).

on the CPW arms. The corresponding line characteristic impedances of slotline and CPW branch arms for 3 dB coupling, in terms of the termination impedance Z_0, can be expressed as

$$Z_{\mathrm{CPW}} = Z_0/\sqrt{2}; \quad Z_S = Z_0 \tag{2}$$

where Z_{CPW} is the impedance of the CPW arms, and Z_S is the impedance of the slotline shunt branch arms. According to the Eq. (2), a truly uniplanar hybrid branch-line coupler was built on a 1.27-mm-thick RT/Duroid ($\epsilon_r = 10.8$) substrate. To test the hybrid branch-line coupler, the wide-band slotline-CPW transitions shown in Fig. 4(b) was connected ports 1, 2, 3, and 4. The measurements were performed on an HP-8510 network analyzer using standard subminiature (SMA) connectors. The performance includes two coax-CPW transitions and two CPW-slotline transitions. Figure 14(c) shows the measured frequency responses of the hybrid branch-line coupler. Over a 40% bandwidth centered at 3 GHz, the power dividing balance and phase difference between ports 2 and 3 are ± 1 dB and $83° \pm 3°$, respectively. The isolation between ports 1 and 4 is greater than 20 dB, and the return loss is more than 19 dB over the same bandwidth. This slotline-CPW hybrid branch-line coupler exhibits superior broad-band performance over conventional microstrip branch-line couplers.

De Ronde's Couplers. In 1970 de Ronde proposed a new coupler and has been named after him. The de Ronde coupler is particularly suitable for tight coupling like 3 dB hybrids in MIC technology. The coupler configuration consists of a microstrip-slotline coupling section (with a strip on top of the substrate and a slot in the ground plane) connected by four microstrip output lines as shown in Fig. 15(a). An analysis of the coupler has been made by Schiek (12) with the aid of the equivalent transmission line model of the hybrid branch-line coupler. From this design theory, an empirical de Ronde's 3 dB coupler was built at X-band with a measured performance as shown in Fig. 15(b) which is close to the expected behavior. A complete analysis of de Ronde's coupler has been carried out by Hoffman and Siegl (13) using the method of the even-odd mode of four-port network with double symmetry. The scattering parameters of the couplers were derived and the compensated couplers were also demonstrated. In 1995, Ho et al. (14) presented a uniplanar de Ronde's CPW-slot directional coupler. The new coupler uses parallel and series CPW-slotline connections. Both the CPW and slotline are on the same side of substrate. A truly uniplanar de Ronde's CPW-slot directional coupler with 5 dB coupling was demonstrated for use from 2.4 GHz to 3.4 GHz.

Figure 16(a) shows the physical configuration of the uniplanar de Ronde's CPW-slot directional couplers (16). The couplers consist of a section of CPW and slotline which are in close proximity and are continuously coupled. The slotline coupling section with a compensation length L_S is terminated with a slotline radial stub on both ends, as shown in Fig. 16(a). The purpose of adding an extended slotline section L_S is to compensate for the difference of phase velocity between the even- and odd-mode coupling. The output four ports are formed by two CPW-slotline tee junctions. Figure 16(b) shows the equivalent transmission line model of the coupler.

To test the coupler, a wide-band CPW-slotline transition was used to connect to ports 1, 2, 3, and 4. The measurements were made using standard SMA connectors and an HP-8510 network analyzer. Experimental results showed that the uniplanar de Ronde's coupler achieved a greater than 30% bandwidth from 2.4 GHz to 3.4 GHz, a power coupling of 5.5 dB (including insertion loss), a more than 14 dB return loss, greater than 17 dB isolation, and $90° \pm 4°$ phase difference between ports 2 and 3. The poor return loss is due to the mechanical tolerances, misalignments, and connectors.

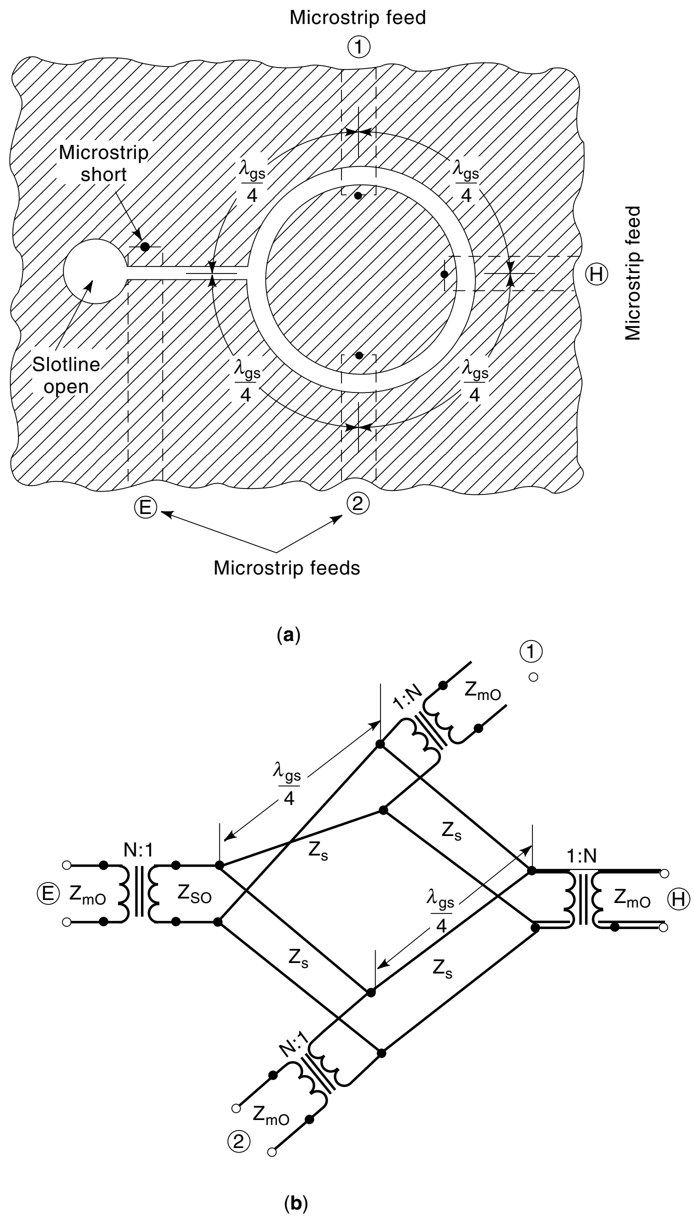

Figure 19. Double-sided slotline magic-T with microstrip feeds: (a) physical configuration; (b) equivalent circuit. (From K. Chang, *Microwave Ring Circuits and Antennas,* 180 degree double-sided slotline ring magic-Ts, New York: Wiley & Sons, p 203, © 1996. Reprinted by permission of John Wiley & Sons, Inc.)

180° Reverse-Phase Hybrid-Ring Couplers. The microstrip rat-race hybrid-ring has been widely used in microwave power dividers and combiners. Figure 17(a) shows the physical configuration of the hybrid-ring coupler consisting of

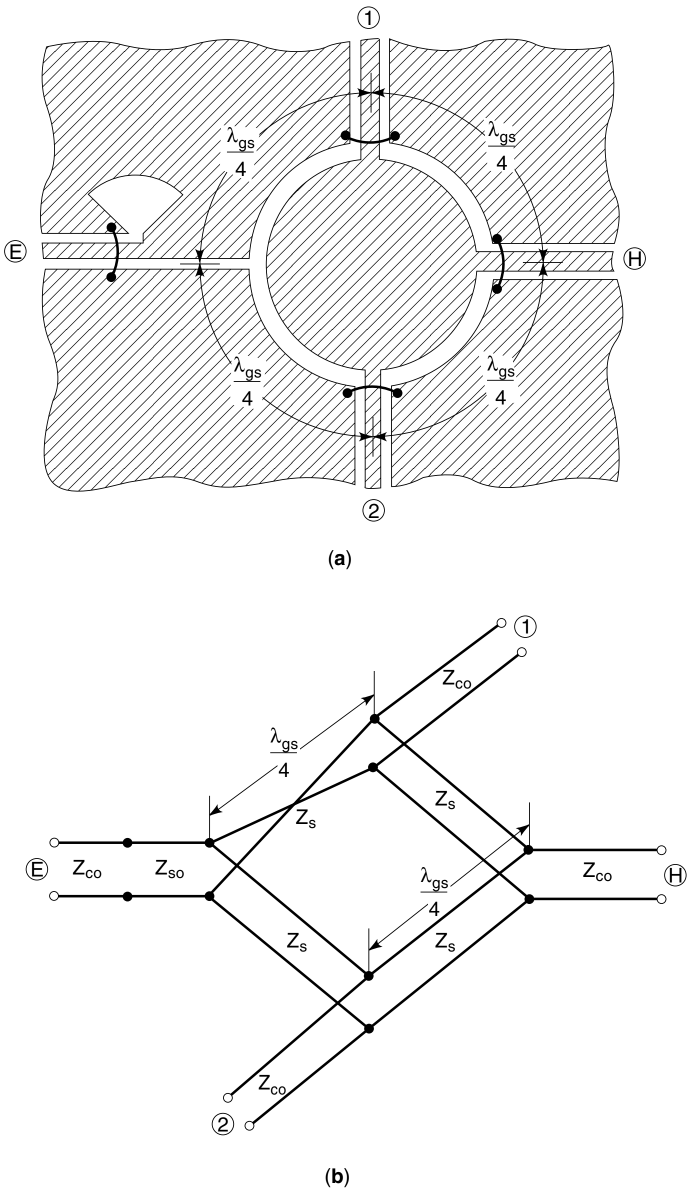

Figure 20. Uniplanar slotline magic-T using a 180° reversed-phase slotline T-junction: (a) physical configuration; (b) equivalent transmission line model. (From K. Chang, *Microwave ring circuits and antennas,* 180 degree double-sided slotline ring magic-Ts, New York: Wiley & Sons, pp 207–208, © 1996. Reprinted by permission of John Wiley & Sons, Inc.)

three $\lambda_m/4$ sections, $3\lambda_m/4$ delay section, and four microstrip T junctions. Typically this coupler has a bandwidth of 20% to 25%. To extend the bandwidth, a modified version of this coupler was proposed by Chua in 1971 (15). This modified reverse-phase hybrid-ring coupler used a $\lambda_S/4$ section of a pair of microstrip-slotline transitions to replace the $3\lambda_m/4$ section of the conventional $3\lambda_m/2$ microstrip rat-race hybrid-ring coupler as shown in Fig. 17(b). The microstrip-slotline transitions provide a remaining 180° phase delay. Since the phase change of the microstrip-slotline transition is frequency independent, the resulting reverse-phase hybrid-ring coupler has a bandwidth of greater than an octave. Although the modified version gives good performance with a wide bandwidth, the double-sided implementation of a curved $3\lambda_m/4$ microstrip line with an inserted $\lambda_S/4$ slotline is not easy for the photolithography process. Also, ground pins are needed for the microstrip shorts.

Recently, uniplanar transmission lines have emerged as alternatives to microstrip in planar microwave integrated circuits. A narrow band uniplanar hybrid coupler was proposed by Hirota et al. in 1987 (16). The circuit is based on a slotline ring with three in-phase CPW feeds via an air bridge. More recently, a broadband uniplanar hybrid-ring coupler (5) operating over an octave bandwidth was developed using a one-wavelength cross-over slotline ring and a one-wavelength crossover CPW ring structure. However, these devices consist of $\lambda/4$ sections that occupy large areas in MIC applications

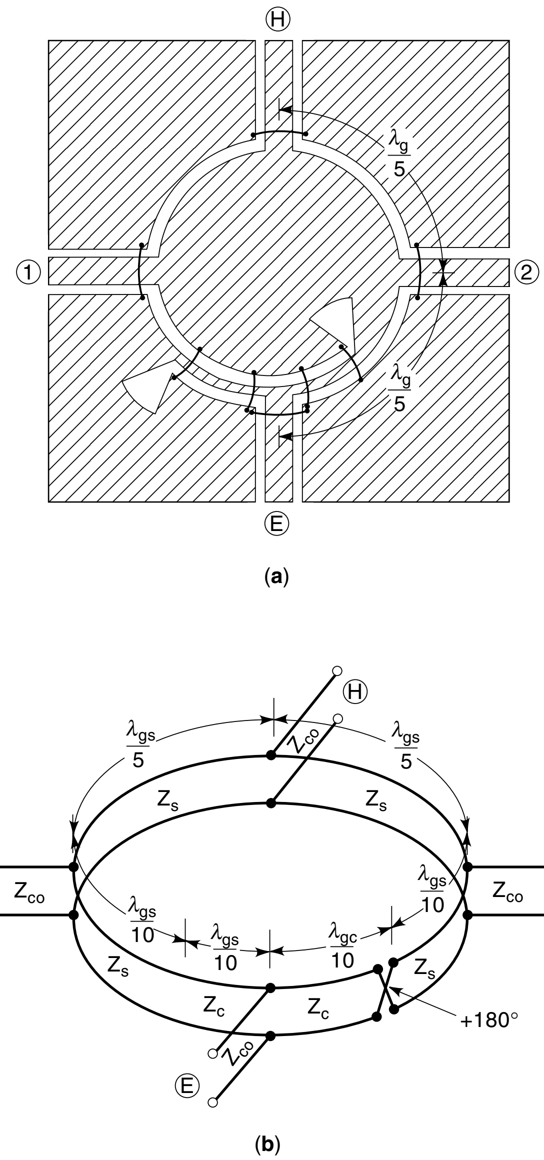

Figure 21. Reduced-size uniplanar hybrid magic-T using a $4\lambda_g/5$ circumference CPW-slotline ring that is 20% smaller than comparable designs: (a) circuit configuration; and (b) equivalent transmission line model. The Magic-T has a bandwidth of 1.6 octave centered at 4 GHz with a 0.4 dB power dividing imbalance and a 2.5° phase imbalance. (From Ref. 17 with permission, © 1995 IEEE.)

and the bandwidth is limited by the electrical line length. To overcome these problems for monolithic integration, a uniplanar reverse-phase hybrid-ring coupler (17) was proposed using a slotline-CPW ring with a 180° reverse-phase slotline-CPW back-to-back balun and four CPW feeds as shown in Fig. 18(a). The circuit consists of four CPW-slotline tee junctions and one 180° reverse-phase slotline-CPW back-to-back balun which is formed using a pair of slotline-CPW transitions. Figure 18(b) shows the equivalent transmission line model. The twisted transmission line represents the 180° reverse-phase CPW-slotline balun. The characteristic impedance of slotline Zs and CPW Zc in terms of CPW feed line impedance Z*co* and θ are given by

$$Z_S = Z_c = Z_{co}\sqrt{2(1-\cot^2\theta)} \tag{3}$$

In this design, $\theta = 72°$ (i.e. $\lambda_{gs}/5$) was chosen resulting in the characteristic impedances Z_S and $Z_c = 66.9\ \Omega$. The hybrid-ring coupler was fabricated on a 1.524 mm-thick RT/Duroid 6010 ($\epsilon_r = 10.5$) substrate. Experimental measurements presented in Fig. 18(c) show that the hybrid-ring coupler has a 1.3 octave bandwidth centered at 4 GHz, a maximum power dividing imbalance of 0.4 dB, and a 2.5° maximum phase imbalance. Compared to microstrip reverse-phase hybrid-ring coupler, the reduced-size slotline-CPW hybrid-ring coupler has the advantages of uniplanar structure, small size, and broadband operation.

Magic Tees. Magic tees are widely used as 0° and 180° power dividers or combiners in microwave circuits such as balanced mixers, balanced amplifiers, and frequency discriminators. The matched waveguide double-T is a well known and commonly used waveguide magic-T. In 1964, Kraker (18) first proposed a planar magic-T which uses an asymmetric coupled transmission line directional coupler and Shiffman's phase-shift network (19). In 1980, Aikawa and Ogawa (20) proposed a double-sided magic-T that is constructed with microstrip-slotline T-junctions and coupled slotlines. The two balanced arms of the double-sided magic-T are on the same side and they do not need a crossover connection. The double-sided magic-T has a bandwidth from 2 GHz to 10 GHz. In recent years, uniplanar magic-Ts have been preferred for planar microwave integrated circuits because they allow easy series and shunt connections of passive and active solid-state de-

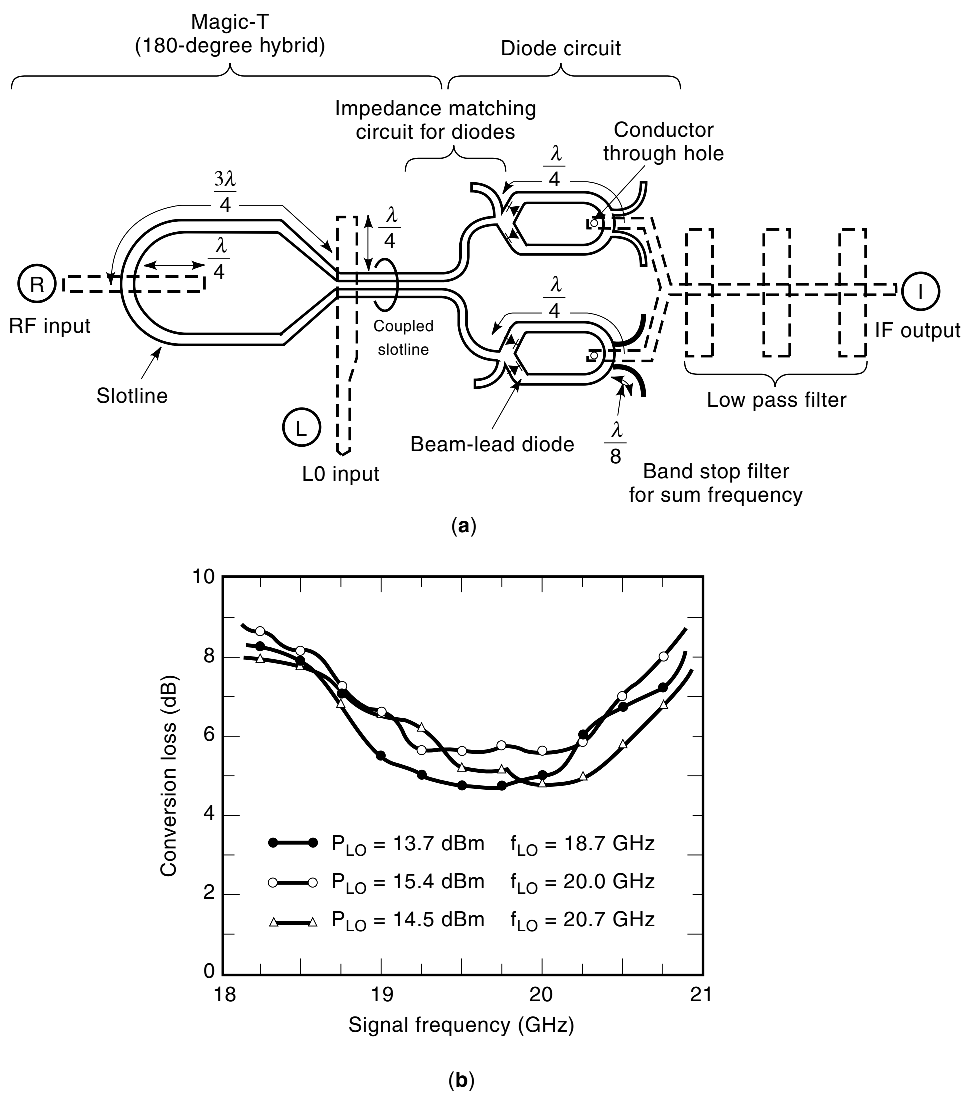

Figure 22. (a) Physical configuration of double-balanced mixer. Solid lines show slotlines and coupled slotlines on the substrate. Dotted lines show microstrip lines on the back side of the substrate. (b) Conversion loss of the mixer. (From Ref. 23 with permission, © 1980 IEEE.)

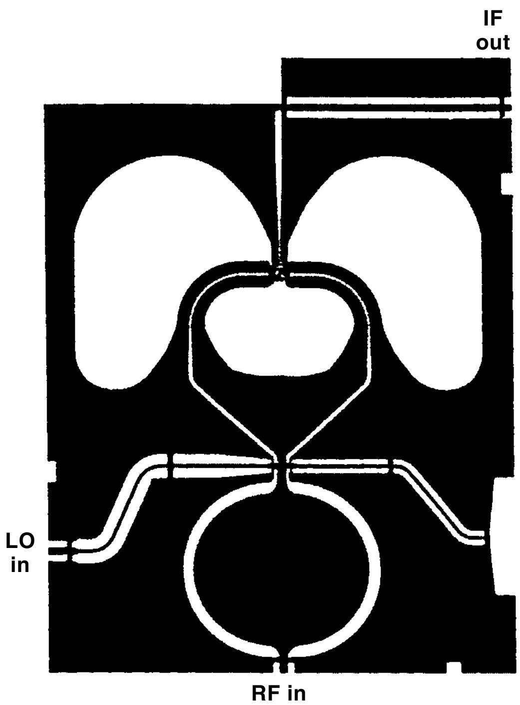

(a)

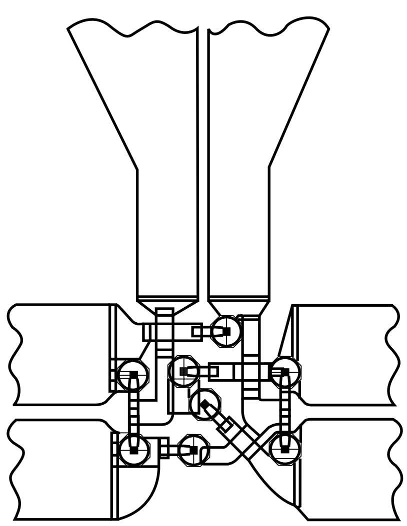

(b)

Figure 23. Double-double balanced mixer: (a) photograph of the circuit, chip size is $4.57 \times 6.1 \times 0.4\ \text{mm}^3$; (b) detail of dual diode ring connection to the circuit. (From Ref. 24 with permission, © 1991 IEEE.)

vices without via holes. In 1987, Hirota et al. (16) proposed a uniplanar magic-T that uses three CPW-slotline T-junctions and a slotline T-junction. The in-phase CPW excitation is via an air bridge and the slotline T-junction is used as a phase inverter. The uniplanar magic-T has a narrow bandwidth. The next presents a double-sided slotline magic-T (21), then a uniplanar slotline magic-T will be discussed (22). These two magic-Ts are based on a 180° phase-reversal of the slotline T-junction as shown in Fig. 1(e). Finally, a reduced-size uniplanar magic-T will be discussed (17) with its equivalent circuit. Since the out-of-phase CPW-slotline T-junction is basically frequency independent, the resulting magic-T has a broad bandwidth with good performance.

180° Double-Sided Slotline Magic-T. Figure 19(a) shows the circuit configuration of the double-sided slotline magic-T (21). The circuit simply consists of a slotline T-junction connected to a slotline-microstrip transition and a slotline ring with three microstrip feeds. The slotline T-junction is a well-known 180° reverse-phase T-junction and is used as a phase inverter in the slotline magic-T. In Fig. 19(a), ports E and H correspond to the E- and H-arms of the conventional waveguide magic-T, respectively. Ports 1 and 2 are the power-dividing balanced arms. The equivalent transmission line model of the slotline magic-T is shown in Fig. 19(b). The twisted transmission line represents the phase reversal of the slotline T-junction. The characteristic impedance of the slotline Z_S in terms of the input-output characteristic impedance Z_{S0} is given by $Z_S = \sqrt{2}\, Z_{S0}$. The radius of the slotline ring is determined by $2\pi r = \lambda_{gs}$, where λ_{gs} is the guide wavelength of the slotline ring. The test circuit was built on a RT/Duroid 6010.8 substrate ($\epsilon_r = 10.8$, $h = 1.27$ mm). Measured results show that the slotline magic-T has an excellent isolation of greater than 35 dB and a good power-dividing balance of 0.2 dB over an 80% bandwidth. The calculated results from the equivalent model agreed very well with the measured data.

180° Uniplanar Slotline Magic-T. Figure 20 shows the physical configuration of the uniplanar slotline magic-T and its equivalent circuit (16). Similar to the double-sided slotline magic-T, the E-arm of the uniplanar magic-T is fed through a slotline connected to a broad-band slotline-CPW transition. The slotline T-junction is used as a phase inverter to achieve the 180° phase reversal. The H-arm and output balanced arms are all fed by CPW lines. This uniplanar slotline magic-T also has good performance over a bandwidth of one octave from 2 GHz to 4 GHz with ±0.25 dB power dividing balance and ±1° phase balance.

Reduced-Size Uniplanar Magic-T. Figure 21(a) shows the circuit configuration of the magic-T consisting of one out-of-phase and three in-phase CPW-slotline T-junctions (17). The out-of-phase T-junction serves as a phase inverter. In Fig. 21(a), ports E and H correspond to the E- and H-arm of the conventional waveguide magic-T, respectively. Ports 1 and 2 are the balanced arms. Figure 21(b) shows the equivalent

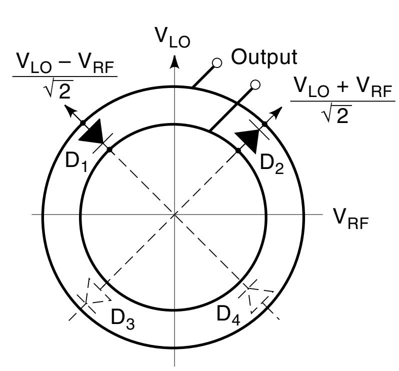

Figure 24. Quasi-optical slotline ring mixer. Four diodes are separated by 90° along the ring, and the basic operation of the mixer is in a balanced polarization-duplexed mode. (From Ref. 25 with permission, © 1983 IEEE.)

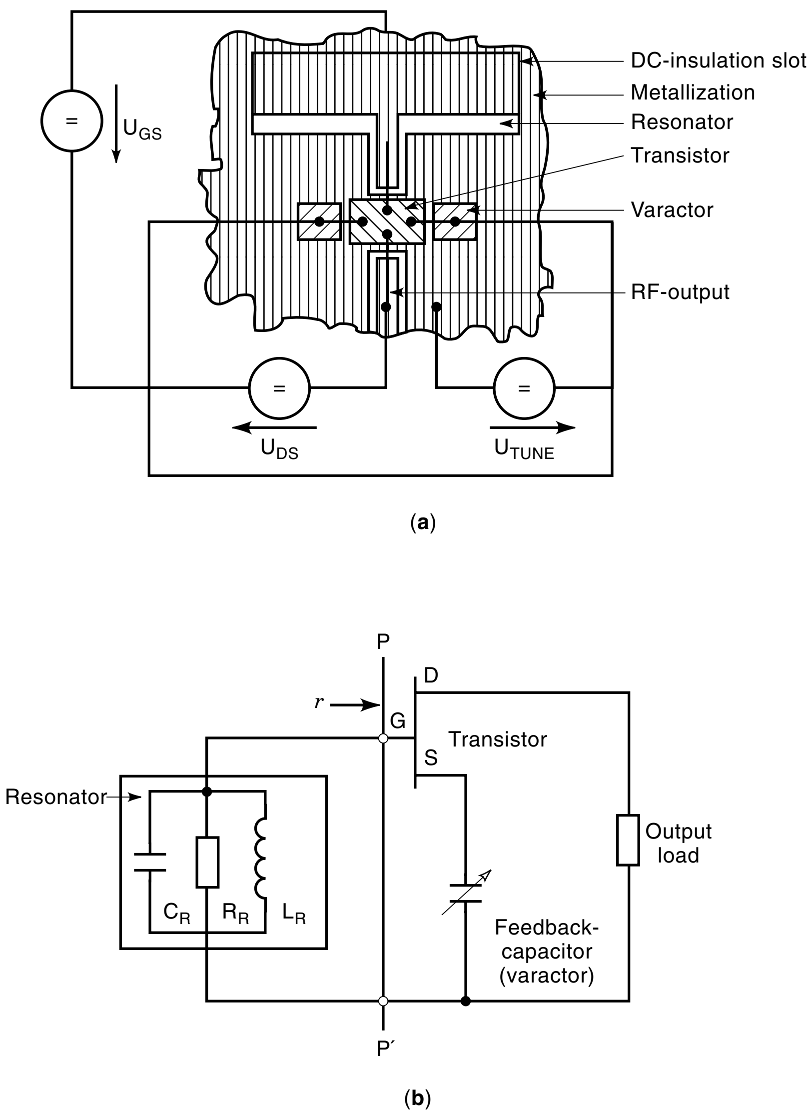

Figure 25. MMIC varactor-tuned oscillator using slotline resonator: (a) physical configuration; and (b) equivalent circuit for the calculation of the RF behavior. (From Ref. 26, reprinted with permission from *Microwave Journal,* Sept. 1990, p 223.)

transmission line model of the magic-T. The twisted transmission line represents the phase reversal of the CPW-slotline T-junction.

SOLID-STATE INTEGRATED CIRCUITS (ACTIVE COMPONENTS) USING SLOTLINES

This section presents various microwave integrated circuits such as mixers, oscillators, modulators, and frequency doublers constructed by using slotlines or the combination of the slotlines and other transmission lines with solid-state devices. A few quasi-optical circuits integrated with slotline antennas are also briefly described.

Mixers

There are three basic types of mixer circuits: single-ended, single-balanced, and double-balanced which are commonly used in microwave applications. Some examples of planar mixer circuits with slotline follow.

Double-Balanced Mixer. In 1980, Ogawa et al. (23) described a MIC double-balanced mixer. The mixer consists of a magic-T for combining the radio frequency (RF) and local oscillation (LO) signals, and a balun transition circuit for separating the RF(LO) and intermediate frequency (IF) signals as shown in Fig. 22(a). These circuits are constructed by using combinations of microstrip lines, slotlines, and coupled slotlines, together with four beam-lead Schottky-barrier diodes. In Fig. 22(a) through the magic-T, the RF and LO signals are supplied to two pairs of diodes in phase and 180° out of phase, respectively. The IF signal is derived from port I composed of a microstrip low-pass filter which is used to suppress undesired signals. The diode circuit in Fig. 22(a) consists of two impedance-matching slotline sections, four $\lambda/4$ slotlines, two pairs of beam-lead diodes, six $\lambda/8$ slotline shorted-stubs, and two cylindrical conductors used for connecting slotlines and microstrip lines through holes in the substrate. These $\lambda/4$ slotlines are used to utilize effectively the RF and LO powers fed to the diodes. The six $\lambda/8$ slotline shorted stubs serving as band stop filters are connected to the slotlines in order to suppress the sum frequency.

The double-balanced mixer was fabricated on a 0.3-mm thick alumina substrate with a dielectric constant of 9.6. Figure 22(b) shows the measured conversion loss for several LO frequencies. The minimum conversion loss of the mixer is 4.7 dB at a signal frequency of 9.6 GHz, and isolation between the three ports is greater than 20 dB from 18 GHz to 21 GHz. This type of double-balanced mixer can be easily fabricated using ordinary MIC techniques and can be applied to other balanced devices like balanced modulators and upconverters.

Uniplanar Double-Double-Balanced MMIC Mixer. An arrangement for a double-double-balanced mixer (DDBM) using slotlines, coplanar waveguides (CPW), and coplanar strips (CPS) is shown in Fig. 23 (24). The DDBM is composed of a 180° hybrid, an IF balun, and eight GaAs Schottky diodes. The circuit uses a balanced LO input and an unbalanced RF input. The LO signal is applied to the difference part and the RF signal is fed to the sum port. The 180° hybrid couples the RF signal in phase and LO signal opposite phase to the diodes. Matching between the hybrid and diodes is accomplished by a slotline section and a CPS section in cascade. The IF output is through the IF balun consisting of a CPW-slotline transition followed by a slotline-CPS transition.

The MMIC mixer was fabricated on a 0.4-mm thick GaAs substrate without the use of via holes. The resulting DDBM operated over a RF bandwidth of 6 GHz to 20 GHz, a LO bandwidth of 8 GHz to 18 GHz, and IF bandwidth of 2 GHz to 7 GHz with conversion loss ranging from 6.2 dB to 9.8 dB. Isolation between the three ports were all greater than 20 dB. The mixer was analyzed using the harmonic balance method, and the measured and simulated results were in reasonable agreement.

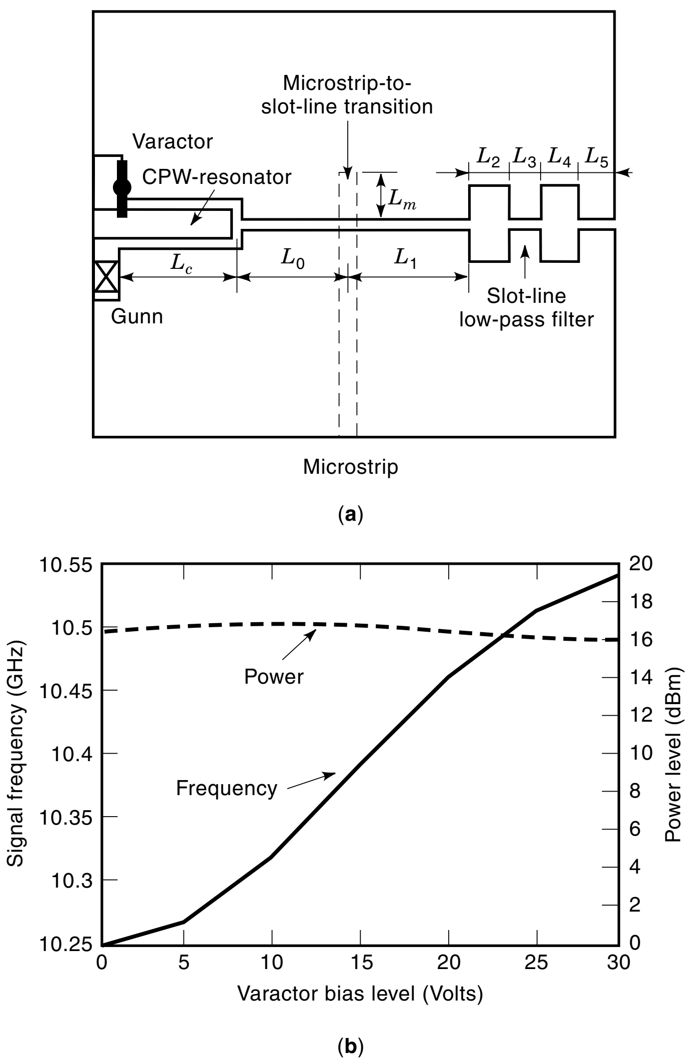

Figure 26. Varactor-tuned CPW/slotline Gunn oscillator: (a) physical configuration; (b) varactor bias voltage versus frequency and power output. Packaged Gunn (MA49106) and varactor (MA46602F) diodes from M/A COM were used for the circuit integration. The circuit was fabricated on a 0.635 mm thick RT/Duroid 6010 substrate (ϵ_r = 10.5). (From Ref. 27 with permission, © 1991 IEEE.)

Quasi-Optical Slotline Ring Mixer. The slotline ring discussed in the previous section was also used as an antenna to build a quasi-optical mixer (25). Figure 24 shows the circuit arrangement. The RF signal arrives as a horizontally polarized plane wave incident perpendicular to the antenna. The LO signal is vertically polarized, and can arrive from either side of the structure. V_{LO} and V_{RF} are the electric field vectors on the antenna plane. By resolving each vector into two perpendicular components, it is easy to see that the mixer diode D_1 receives $(V_{LO} - V_{RF})/\sqrt{2}$, while D_2 receives $(V_{LO} + V_{RF})/\sqrt{2}$. In effect, each diode has its own independent mixer circuit with the intermediate frequency (IF) outputs added in parallel. The IF signal appears as a voltage between the central metal disk and the surrounding ground plane and is removed through an RF choke. A double-balanced mixer with improved isolation can be made by adding two additional diodes D_3 and D_4, as indicated.

The antenna-mixer has good LO-to-RF isolation because of the symmetry provided by the balanced configuration. A conversion loss of 6.5 dB was measured for this quasi-optical mixer operating at X-band.

Oscillators

Oscillators are one-port circuits generating sinusoidal signals, and are widely applied in microwave transmission and measurement systems. Early oscillator circuits were made using waveguide or coaxial-line technology. Modern designs are often made in planar technology such as microstrip, CPW, slotline, and their combination technologies as well as MIC and MMIC technologies. Examples of oscillator circuits using slotlines follow.

MMIC Varactor-Tuned Oscillator Using a Slotline Resonator. Varactor-tuned oscillators provide more constant output power, wider tuning range, and faster response than those of bias tuning oscillators. Figure 25(a) shows an MMIC varactor-tuned oscillator using a slotline resonator proposed by Roth et al. (26) in 1990. The oscillator was driven by a GaAs field-effect transistor (FET) connected in common source with a capacitive serial feedback. Coupling was realized by a GaAs varactor integrated on the same substrate with the FET. A slotline resonator was built as a linear resonator with coplanar waveguide (CPW) coupling to the FET gate. Bonding wires were used to connect the circuit elements while the output CPW connection was made with a microwave probe. The equivalent circuit of the oscillator as shown in Fig. 25(b) was

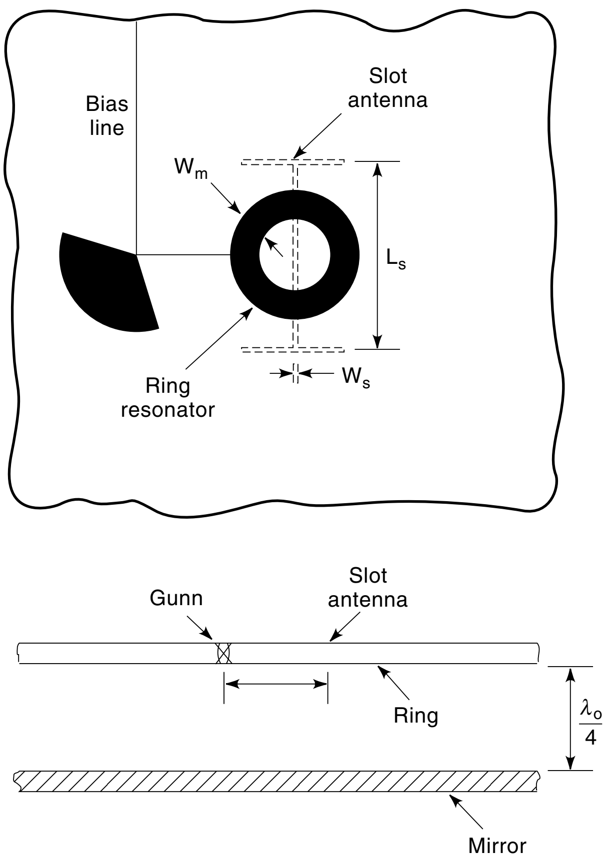

(**a**)

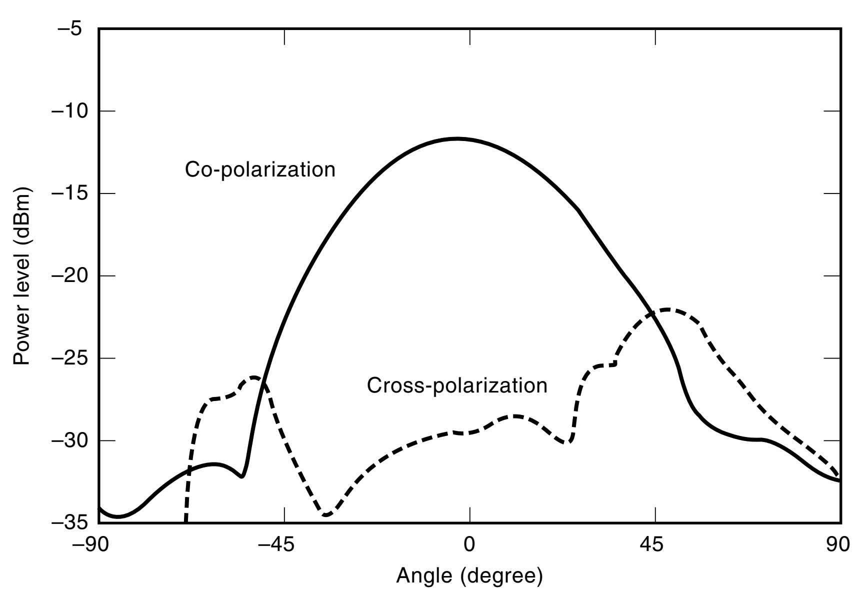

(**b**)

Figure 27. Gunn oscillator driving slot antenna: (a) circuit configuration; (b) H-plane pattern of the antenna. The antenna circuit was fabricated on RT/Duroid 5880 dielectric substrate of ϵ_r = 2.20 and thickness h = 1.57 mm with Gunn diodes of model number MA49135 from M/A COM. (From Ref. 28 with permission, © 1995 IEEE.)

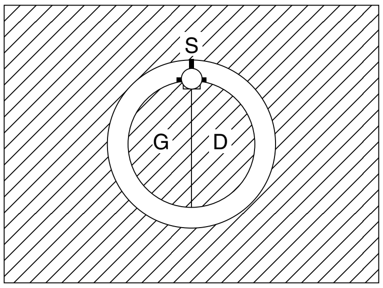

Figure 28. Circuit configuration of an FET active slotline ring antenna. The circuit was etched on RT/Duroid 5870 board with the following dimensions: relative dielectric constant $\epsilon_r = 2.20$; substrate thickness h = 1.57 mm; inner radius of the slotline ring $d_i = 9.54$ mm; and outer radius of the slotline ring $d_o = 11.54$ mm. The active device used in the circuit is an Avantek ATF-26836 FET. (From Ref. 29 with permission from *Electronics Letters.*)

used for circuit simulation and predicting circuit performance. The capacitive serial feedback of the FET provides a reflection coefficient r greater than unity in the plane p-p'. The resonant frequency was determined by the resonant circuit and the feedback varactor. A test circuit was fabricated and measured. A tuning range of nearly one octave was achieved with 10 mW output power. The experimental results had good agreement with the calculated electrical properties.

Another varactor-tuned oscillator driven by a Gunn diode was built on CPW and slotline (27) as shown in Fig. 26(a). The circuit consists of a Gunn diode, a varactor diode, a CPW resonator, a slotline low-pass filter for RF choke and diode biases, and a slotline-microstrip transition for coupling power to output. This VCO provides 16.3 dB ± 0.35 dB output power throughout a 350 MHz tuning range centered at 10.37 GHz. Figure 26(b) shows the power output as a function of frequency and varactor bias. The output power is fairly constant over the tuning range.

Active Slot Antennas Driven by Oscillators. Slot resonators have been used as radiators for antenna applications. A ring-stabilized Gunn oscillator coupled with a slot radiator to form an active antenna was recently reported (28). The circuit configuration is shown in Fig. 27(a). A circular microstrip ring is used as the resonant element of the oscillator. A slot on the ground plane of the substrate coupled with the microstrip ring served as the radiating element. A Gunn diode is mounted between the ring and the ground plane of the substrate at either side of the ring. A metal mirror block is introduced one-quarter wavelength behind the ring to avoid any back scattering. The operating frequency of the active antenna was designed to be close to the first resonant frequency of the circular microstrip ring. A radiated power of 16 dBm at 5.5 GHz was obtained with the bias level of 12.6 V. The H-plane radiation patterns are shown in Fig. 27(b).

An FET oscillator integrated with a slotline ring antenna was also developed (29). Figure 28 shows the physical configuration. A simple transmission line method was used to predict the resonant frequency. The FET oscillator driven slotline antenna radiated 21.6 mW at 7.7 GHz with 18% DC to RF efficiency.

Modulators

A number of digital modulators have been developed for digital communication systems. Digital modulators are classified into three types: the amplitude-shift-keying (ASK) modulator, the phase-shift-keying (PSK) modulator, and the frequency-shift-keying (FSK) modulator. The basic information about modulation can be found elsewhere in this encyclopedia (see the article MODULATION ANALYSIS FORMULA). Here we introduce some examples of modulator circuits using slotlines.

ASK Modulator Using Double-Sided MIC. There are three types of ASK modulators: reflection, transmission, and balanced. Reflection-type modulators need circulators to separate input and output power or hybrid couplers to maintain perfect matching, while transmission-type modulators use isolators instead of circulators. Balanced-type modulators require balanced/unbalanced hybrid transitions for transforma-

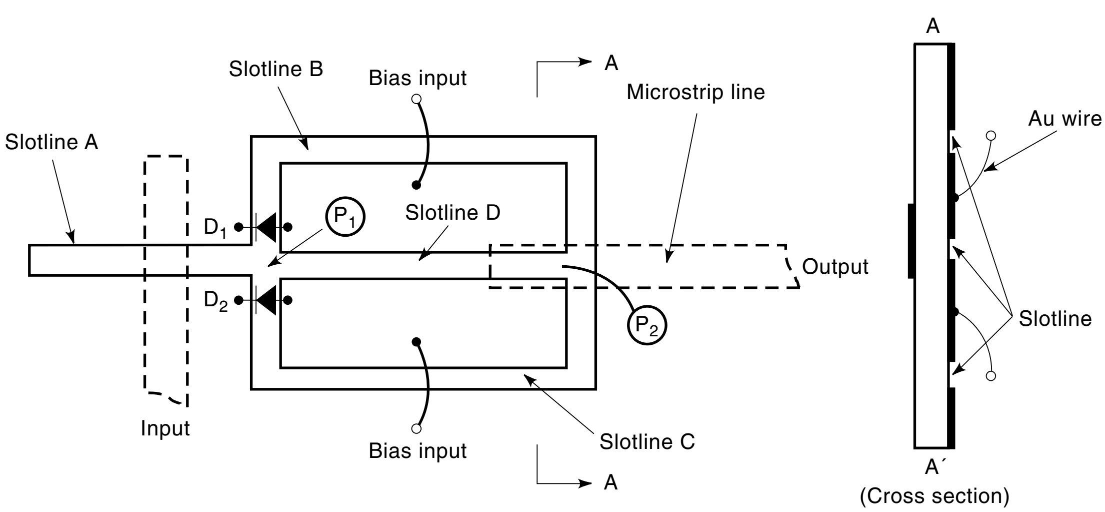

Figure 29. Circuit configuration of the balanced ASK modulator. Solid lines represent slotlines on the substrate. Dotted lines show microstrips on the back side of the substrate. (From Ref. 30 with permission, © 1987 IEEE.)

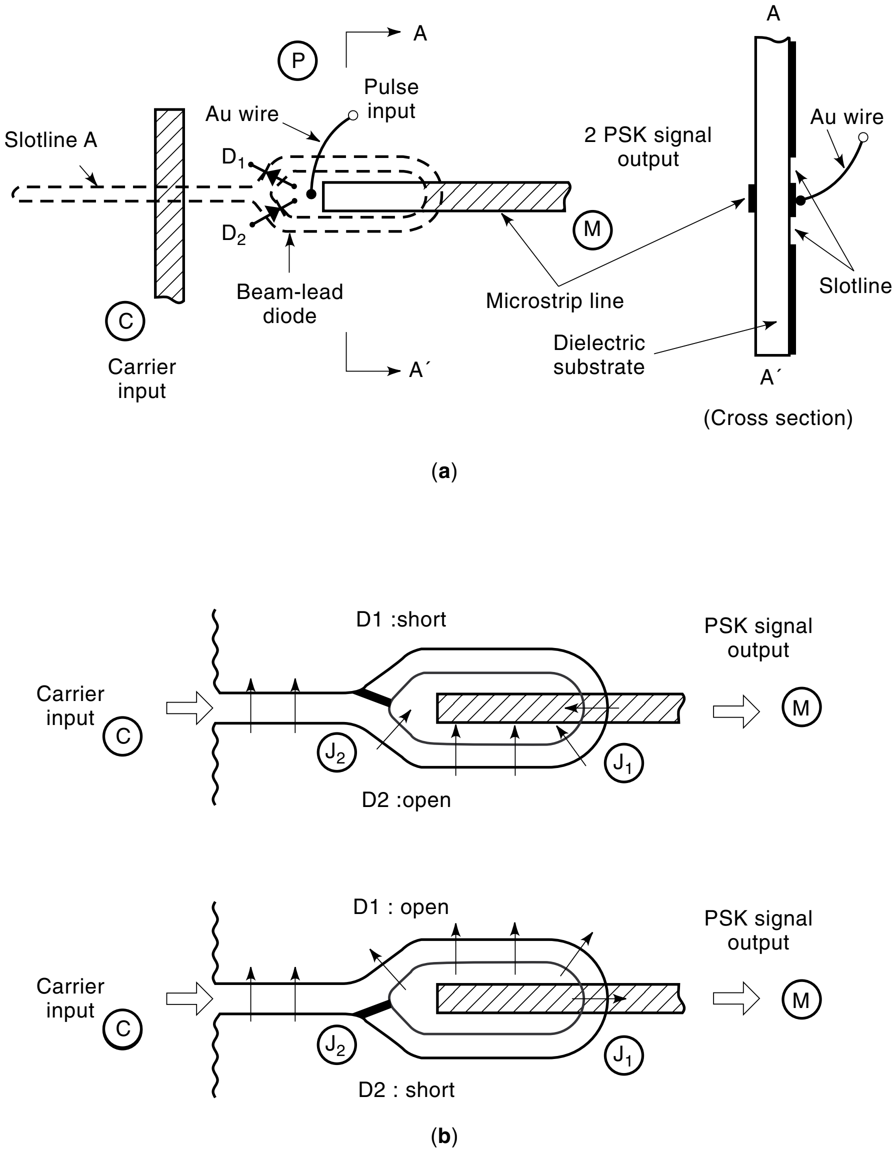

Figure 30. (a) Circuit configuration; and (b) operating principle of balanced biphase-shift-keying (BPSK) modulator. (From Ref. 31 with permission, © 1982 IEEE.)

tion from unbalanced modes to balanced modes, or vice versa. Generally, nonreciprocal components or the matching resistance are necessary to implement ASK modulators.

In 1989, an ASK modulator that does not require circulators and matching resistances was proposed (30). The circuit using double-sided (slotlines and microstrips) MIC is shown in Fig. 29. It consists of two $\lambda/4$ slotlines, a slotline-microstrip transition, and two beam-lead p-i-n diodes. The measurements for the ASK modulator were performed in the frequency range from 25.0 GHz to 29.5 GHz. A 2.8 dB insertion loss, a 12 dB return loss, and an on/off ratio of greater than 40 dB were obtained. This balanced ASK modulator had more compact size than that of other types of ASK modulators because no circulators and hybrid couplers were needed, and it had a fairly high on/off ratio because of the balanced circuit configuration.

Integrated Balanced Biphase-Shift-Keying (BPSK) and Quadriphase-Shift-Keying (QPSK) Modulators. PSK modulators have two types of reflection and transmission (balanced). The basic principle of the reflection-type PSK modulators is similar to that of the ASK modulators. Transmission-type PSK modulators use the difference in path lengths for carriers. By selecting a quarter wavelength for the carrier path line, a 0°–180° (BPSK) modulator can be produced. If a one-eighth wavelength of the carrier line is selected a 0°–90° (QPSK) modulator can be obtained.

Balanced BPSK Modulators. Balanced BPSK modulators are commonly used as digital modulators. Figure 30(a) shows the circuit configuration of a single-balanced BPSK modulator which was proposed (31) for use in Ka-band. The circuit consists of two $\lambda/4$ slotlines, two switching diodes, two slotline-microstrip transition, and a gold wire use to supply modulating pulses to the diodes. The BPSK modulator operates as shown in Fig. 30(b). The arrows represent the electric field of the carrier propagating along the slotlines. When the carrier is supplied to port C the bias states of the diodes determine which path the carrier takes as the data alternately switches the diodes on and off. The carrier takes path 1 or path 2, producing a biphase output signal because the direction of the

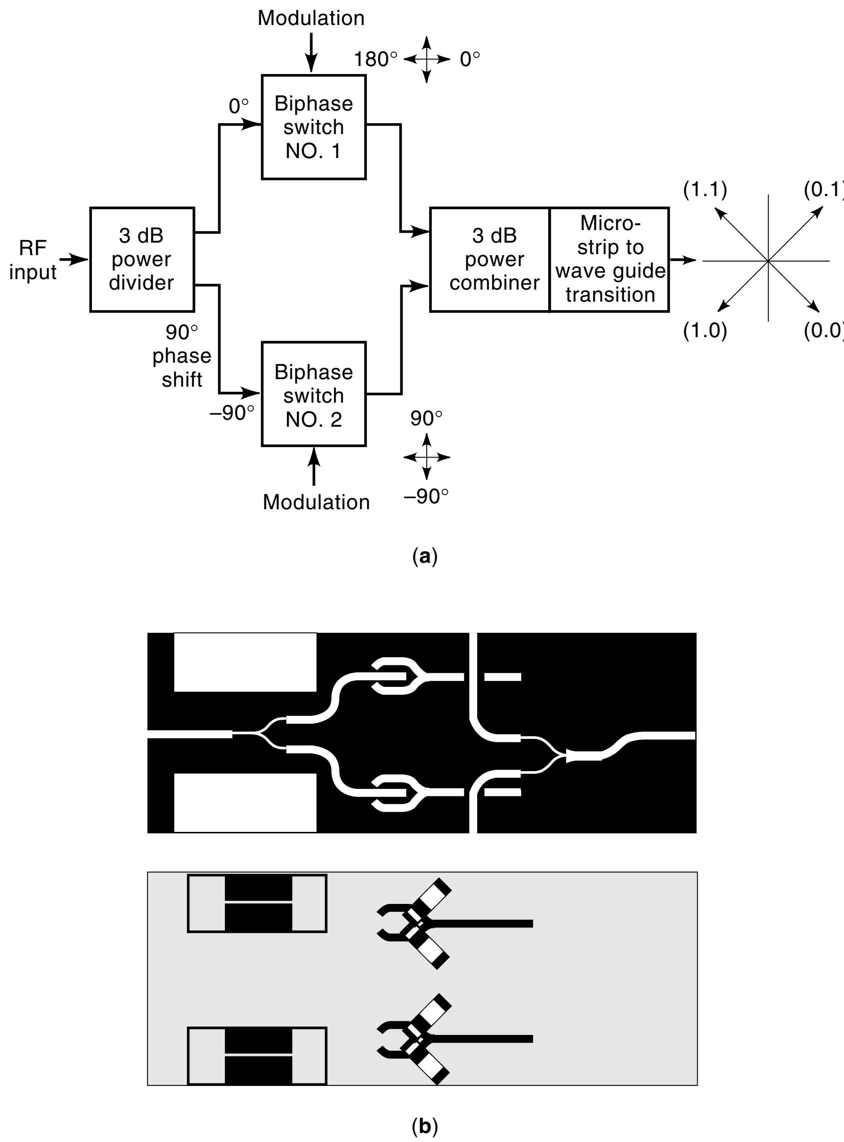

Figure 31. (a) Block diagram; and (b) circuit layout of a quadriphase-shift-keying (QPSK) modulator chip (shown are both sides of the chip). (From Ref. 32 with permission, © 1984 IEEE.)

electric field at the junction J_1 is 180° out-of-phase, as shown in Fig. 30(b). The modulated carrier is then fed to the microstrip port M through the slotline-microstrip transition. The performance of the BPSK modulator has 2.2 dB insertion loss at a carrier frequency of 27 GHz and a greater than 25 dB isolation over a 1 GHz bandwidth. The phase error and amplitude deviation were less than 1° and 0.5 dB, respectively.

Balanced QPSK Modulators. A balanced QPSK modulator is important for digital wireless or satellite communication systems because it allows effective use of frequencies and has also been applied to microwave and millimeter-wave transceivers. A QPSK modulator using double-sided MIC techniques was reported (32) in 1984 for directly modulating a 60-GHz carrier frequency. Figure 31 shows a block diagram and circuit layout of the QPSK modulator. The circuit consists of a Wilkinson power divider with 90° phase shift in one arm, two biphase switches (BPSK modulators) using coupled slot-microstrip structure, and a microstrip-waveguide transition at the output.

The circuit operates as follows. The unmodulated RF carrier enters the circuit on microstrip and goes to the in-phase power divider. The carrier is divided into two signals with equal amplitude and in phase. One arm of the power divider drives the biphase switch No. 1 directly. A 90° phase shifter is introduced at the input of biphase switch No. 2 by increasing the microstrip path length between the power divider and biphase switch No. 2. The biphase switches introduce an additional 0° or 180° phase shift to each signal as the data inputs switch the Schottky diodes. The two biphase-modulated signals are then summed in an in-phase power combiner producing a quadriphase modulated signal. The QPSK modulator has the following design features and advantages:

1. High isolation between the carrier input port and the modulated carrier output port is obtained due to the balanced configuration;
2. A dc return path is not required because slotline is used;
3. The 90° phase shift is introduced by an additional path length instead of using a 90° hybrid (this simplifies the design since a low-loss, well-balanced 90° hybrid is difficult to realize at 60 GHz);

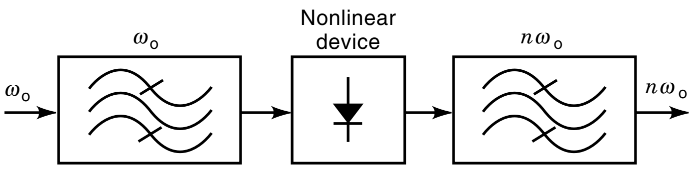

Figure 32. Block diagram of frequency multiplier.

4. The 180° phase shift is introduced by the built-in field distribution of the slotline;
5. A simple configuration using only a wire bonding is sufficient for a baseband input circuit;
6. Small size is achieved by using a sapphire substrate.

The QPSK modulator chip was integrated with a Gunn voltage-control oscillator (VCO), a subharmonic mixer, and a microstrip-waveguide transition to form the RF exciter/modulator module. The modulator demonstrated excellent performance at 60 GHz with an output phase error of less than 3° and maximum amplitude error of 0.5 dB.

Frequency Multiplier

Microwave and millimeter-wave signals can be generated by frequency multiplication of lower frequency signals produced by a quartz-controlled generator. Frequency multipliers are usually used to realize this conversion. Figure 32 shows a block diagram of frequency multiplier. A signal of angular frequency ω_0 is fed to a nonlinear device (varactor diodes or transistors), which generates harmonics at angular frequencies $n\omega_0$. The output signal at the desired frequency is then selected by a bandpass filter. Two examples of quasi-optical frequency multipliers using slot antennas follow.

Quasi-Optical Frequency Multipliers Using Slot Antennas. Using a uniplanar structure of slotline and CPW, a parabola-feed frequency multiplier for millimeter- and submillimeter-wave signal renovation was recently reported (33). The multiplier uses a quad-bridge diode configuration to provide effective isolation between input and output signals. Two pairs of double-slot antennas with orthogonal polarizations directly couple input and output signals to the diodes without the need for hybrid couplers in conventional balanced circuits. Figure 33 shows the circuit configuration of the frequency multiplier implemented on a parabola feed with two pairs of slot antennas. The two input antennas receive a vertically polarized signal in phase while sending the signal to the diodes with opposite phase. The output signal generated by the diodes will be transmitted in phase through the two horizontally polarized antennas. The input and output signals are then coupled to free space by placing the multiplier circuit on an electrically thick substrate lens (a dielectric-filled parabola in this case). This configuration maintains the same conversion efficiency as single-diode multipliers but quadruples the power handing capability. Measurement results of an X- and K-band multiplier show frequency conversion loss of 6.8 dB at the 20.3 GHz output frequency.

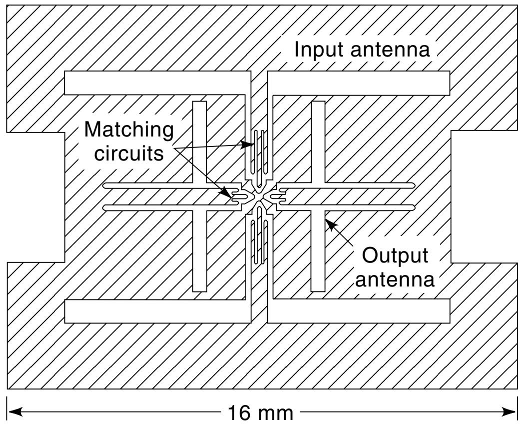

Figure 33. Configuration of an X/K-band quasi-optical frequency multiplier. The circuit is built on a thin quartz substrate and mounted on a stycast-filled ($\epsilon_r = 3.9$) parabola. (From Ref. 33 with permission, © 1997 IEEE.)

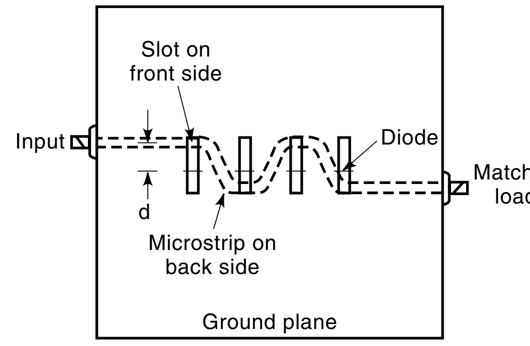

Figure 34. Configuration of frequency multiplier using microstrip-fed slot array. (From Ref. 34 with permission, © 1987 IEEE.)

Another quasi-optical frequency multiplier using double-sided MIC (coupled slot-microscript) techniques was proposed (34) in 1987. The configuration shown in Fig. 34 uses a meander microstrip line to feed an array of diode-loaded slot antennas which are positioned in correct phase to maximize the radiation performance of the multiplier. A 26 dBm, 5.4-GHz input multiplied to 10.8 GHz, was achieved for the circuit. With a planar structure, controllable power coupling, and flexibility in array geometry, the quasi-optical frequency multiplier is suited for MIC and MMIC applications.

BIBLIOGRAPHY

1. K. C. Gupta et al., *Microstrip Lines and Slotlines,* 2nd ed., Norwood, MA: Artech House, 1996.
2. S. B. Cohn, Slot line on a dielectric substrate, *IEEE Trans. Microw. Theory Tech.,* **MTT-17** (10): 768–778, 1969.
3. B. Schuppert, Microstrip/slotline transition: modeling and experimental investigation, *IEEE Trans. Microw. Theory Tech.,* **MTT-36** (8): 1272–1282, 1988.
4. C. H. Ho, L. Fan, and K. Chang, Broad-band uniplanar hybrid-ring and branch-line couplers, *IEEE Trans. Microw. Theory Tech.,* **MTT-41** (12): 2116–2125, 1993.
5. C. H. Ho, L. Fan, and K. Chang, New uniplanar coplanar waveguide hybrid-ring couplers and magic-T's, *IEEE Trans. Microw. Theory Tech.,* **MTT-42** (12): 2440–2448, 1994.
6. K. Chang, *Microwave Ring Circuits and Antennas,* New York: Wiley, 1996.

7. J. A. Navarro and K. Chang, Varactor-tunable uniplanar ring resonators, *IEEE Trans. Microw. Theory Tech.,* **MTT-41** (5): 760–766, 1993.
8. E. A. Mariani and J. P. Agrios, Slot-line filters and couplers, *IEEE Trans. Microw. Theory Tech.,* **MTT-18** (12): 1089–1095, 1970.
9. C. H. Ho, L. Fan, and K. Chang, Slotline annular ring elements and their applications to resonator, filter and coupler design, *IEEE Trans. Microw. Theory Tech.,* **MTT-41** (9): 1648–1650, 1993.
10. G. H. Robinson and J. L. Allen, Slot line application to miniature ferrite devices, *IEEE Trans. Microw. Theory Tech.,* **MTT-17** (12): 1097–1101, 1969.
11. C. H. Ho, *Slotline, CPW ring circuits and waveguide ring cavities for coupler and filter application,* Ph.D. dissertation, Texas A&M University, College Station, 1994.
12. B. Schiek, Hybrid branchline coupler—a useful new class of directional couplers, *IEEE Trans. Microw. Theory Tech.,* **MTT-22** (10): 864–869, 1974.
13. R. Hoffmann and J. Siegl, Microstrip-slot coupler design—Part I and Part II, *IEEE Trans. Microw. Theory Tech.,* **MTT-30** (8): 1205–1216, 1982.
14. C. Ho, L. Fan, and K. Chang, Uniplanar de Ronde's CPW-slot directional couplers, *IEEE MTT-S Int. Microw. Symp. Dig.,* **3**: 1399–1402, 1995.
15. L. W. Chua, New broad-band matched hybrids for microwave integrated circuits, *Proc. 2nd Eur. Microw. Conf.,* pp. C4/5:1–C4/5:4, 1971.
16. T. Hirota, Y. Tarusawa, and H. Ogawa, Uniplanar MMIC hybrids–a proposed new MMIC structure, *IEEE Trans. Microw. Theory Tech.,* **MTT-35** (6): 576–581, 1987.
17. L. Fan et al., Wide-band reduced-size uniplanar magic-T, hybrid-ring, and de Ronde's CPW-slot couplers, *IEEE Trans. Microw. Theory Tech.,* **MTT-43** (12): 2749–2758, 1995.
18. D. I. Kraker, A symmetric coupled-transmission-line magic-T, *IEEE Trans. Microw. Theory Tech.,* **MTT-12** (11): 595–599, 1964.
19. B. M. Schiffman, A new class of broad-band microwave 90-degree phase shifters, *IRE Trans. Microw. Theory Tech.,* **MTT-6** (4): 232–237, 1958.
20. M. Aikawa and H. Ogawa, A new MIC magic-T using coupled slot line, *IEEE Trans. Microw. Theory Tech.,* **MTT-28** (6): 523–528, 1980.
21. K. Chang, *Microwave Ring Circuits and Antennas,* New York: Wiley, 1996, pp. 202–206.
22. K. Chang, *Microwave Ring Circuits and Antennas,* New York: Wiley, 1996, pp. 207–213.
23. H. Ogawa, M. Aikawa, and K. Morita, K-band integrated double-balanced mixer, *IEEE Trans. Microw. Theory Tech.,* **MTT-28** (3): 180–185, 1980.
24. J. Eisenberg, J. Panelli, and W. Ou, A new planar double-double balanced MMIC mixer structure, *IEEE MTT-S Int. Microw. Symp. Dig.,* **1**: 81–84, 1991.
25. K. D. Stephan, N. Camilleri, and T. Itoh, A quasi-optical polarization-duplexed balanced mixer for millimeter-wave applications, *IEEE Trans. Microw. Theory Tech.,* **MTT-31** (2): 164–170, 1983.
26. B. Roth, M. Joseph, and A. Beyer, A varactor-tuned oscillator using MMIC technology, *Microw. J.,* **33** (9): 223–225, 1990.
27. J. A. Navarro, Y. Shu, and K. Chang, A novel varactor tunable coplanar waveguide-slotline Gunn VCO, *IEEE MTT-S Int. Microw. Symp. Dig.,* **3**: 1187–1190, 1991.
28. Z. Ding, L. Fan, and K. Chang, A new type of active antenna for coupled Gunn oscillator driven spatial power combining arrays, *IEEE Microw. Guided Wave Lett.,* **5** (8): 264–266, 1995.
29. C. H. Ho, L. Fan, and K. Chang, New FET active slotline ring antenna, *Electron. Lett.,* **29** (6): 521–522, 1993.
30. Y. Tarusawa, H. Ogawa, and T. Hirota, A new constant-resistance ASK modulator using double-sided MIC, *IEEE Trans. Microw. Theory Tech.,* **MTT-35** (9): 819–822, 1987.
31. H. Ogawa, M. Aikawa, and M. Akaike, Integrated balanced BPSK and QPSK modulators for the Ka-band, *IEEE Trans. Microw. Theory Tech.,* **MTT-30** (3): 227–234, 1982.
32. A. Grote and K. Chang, 60-GHz Integrated-circuit high data rate quadriphase shift keying exciter and modulator, *IEEE Trans. Microw. Theory Tech.,* **MTT-32** (12): 1663–1667, 1984.
33. M. Kim et al., A planar parabola-feed frequency multiplier, *IEEE Microw. Guided Wave Lett.,* **7** (3): 60–62, 1997.
34. S. Nam, T. Uwano, and T. Itoh, Microstrip-fed planar frequency multiplying space combiner, *IEEE Trans. Microw. Theory Tech.,* **MTT-35** (12): 1271–1276, 1987.

LU FAN
KAI CHANG
Texas A&M University